Biological Sciences – Microbiology

Interplay between tolerance mechanisms to copper and acid stress in *Escherichia coli*

Karrera Y. Djoko*, Minh-Duy Phan, Kate M. Peters, Mark J. Walker, Mark A. Schembri, and Alastair G. McEwan

School of Chemistry and Molecular Biosciences and Australian Infectious Diseases Research Centre,
The University of Queensland,
St Lucia, QLD 4072,
Australia

***Corresponding author**
Mailing address: Bdg 76 Cooper Road, School of Chemistry and Molecular Biosciences, The University of Queensland, St Lucia, QLD 4072, Australia
Phone: (+61) 7 3365 4603
Email: k.djoko@uq.edu.au

Keywords: copper stress and tolerance, UPEC, acid resistance, GOGAT, glutamate biosynthesis

ABSTRACT (217 words)

Copper (Cu) is a key antibacterial component of the host innate immune system and almost all bacterial species possess systems that defend against the toxic effects of excess Cu. The Cu tolerance system in Gram-negative bacteria comprises minimally of a Cu sensor (CueR) and a Cu export pump (CopA). The *cueR* and *copA* genes are encoded on the chromosome typically as a divergent but contiguous operon. In *E. coli*, *cueR* and *copA* are separated by two additional genes, *ybaS* and *ybaT*, which confer glutamine (Gln)-dependent acid tolerance and contribute to the glutamate (Glu)-dependent acid resistance system in this organism. Here we show that Cu strongly inhibits growth of a Δ*copA* mutant strain in acidic cultures. We further demonstrate that Cu stress impairs the pathway for Glu biosynthesis *via* glutamate synthase (GltBD or GOGAT), leading to decreased intracellular levels of Glu. Addition of exogenous Glu rescues the Δ*copA* mutant from Cu stress in acidic conditions. Gln is also protective but this relies on the activities of YbaS and YbaT. Notably, expression of both enzymes is upregulated during Cu stress. These results demonstrate a link between Cu stress, acid stress, and Glu/Gln metabolism, establish a role for YbaS and YbaT in Cu tolerance, and suggest that subtle changes in core metabolic pathways may contribute to overcoming host-imposed copper toxicity.

SIGNIFICANCE STATEMENT (101 words)

Copper is an essential trace metal nutrient in health and is increasingly recognized for its role in the control of infection. The pathogen *Escherichia coli* encounters host niches with mild to high acidity and elevated copper levels. Our study shows that this bacterium can alter its metabolism and harness the amino acid glutamine to suppress the effects of acid stress and copper toxicity. Given the abundance of glutamine in systemic circulation and its importance in the host immune system, our work provides a new insight into the ways in which bacterial pathogens can adapt and survive host-imposed antibacterial strategies.

\body

INTRODUCTION

The efflux of excess transition metal ions such as copper (Cu) is an important feature of bacterial physiology, particularly during the interactions between a bacterial pathogen and its host. Several lines of evidence have established a role for Cu as a host-derived antibacterial agent that contributes to nutritional immunity (1). In turn, the ability to export Cu from the bacterial cytoplasm is now recognised as a key determinant of bacterial virulence (2-5). At the biochemical level, the mechanisms of bacterial Cu export are well understood and, in Gram-negative species, are exemplified by the Cue/Cop regulon in *Escherichia coli* (6). This system consists of a Cu(I)-sensing transcriptional regulator (CueR), which controls expression of a transmembrane efflux pump (CopA) that exports Cu(I) from the cytoplasm to the periplasm and a periplasmic cuprous oxidase (CueO) that converts Cu(I) to the less toxic Cu(II) form.

In the *E. coli* chromosome, *copA* and *cueR* are separated by an operon annotated as *ybaST*, which is encoded in the same orientation as *cueR* and is divergent from *copA* (Fig. 1A). *ybaS* encodes a glutaminase that catalyses the hydrolysis of *L*-glutamine (Gln) to generate *L*-glutamate (Glu) and ammonia (Fig. 1B). The glutaminase activity of YbaS confers Gln-dependent acid tolerance and contributes to the Glu-dependent system for acid resistance (AR) (7, 8). In this AR mechanism, Glu is converted to γ-aminobutyric acid (GABA) by two glutamate decarboxylases (GadA, GadB). This process consumes a proton and raises the cytoplasmic pH (9). The intracellular Glu pool can be replenished if an extracellular supply is present and this import occurs *via* the permease GadC (Fig. 1B). *ybaT* encodes an amino acid

permease that may also contribute to Glu-dependent AR by supplying Gln to YbaS for hydrolysis (Fig. 1B) but its substrate specificity remains to be established .

Here we examine the significance of the synteny of Cu tolerance and acid tolerance genes in relation to *E. coli* physiology. Using a Δ*copA* deletion mutant strain, we show a link between Cu stress, acid stress, and Glu/Gln metabolism, and establish a role for YbaS and YbaT in Cu tolerance. Our results suggest that subtle changes in bacterial metabolism may contribute to overcoming host-imposed copper toxicity during nutritional immunity.

RESULTS

Organisation of *copA* and *cueR* in *E. coli*. The nucleotide sequence of the *copA-ybaST-cueR* locus from *E. coli* was used to query all complete bacterial genome sequences in the NCBI database (see Supporting Methods in the SI Appendix). The search results indicated that the synteny of *copA*, *ybaST*, and *cueR* is unique to *Escherichia* and *Shigella* genera (Fig. S1). In the case of *E. coli*, this gene cluster is part of the core genome (10) and is found in 208/209 complete genomes (>95% sequence conservation), which include strains representative of environmental, commensal, and all pathogenic types.

The *ybaST* insertion is absent from other *Enterobactericeae* such as *Salmonella* and *Klebsiella.* In these organisms, *copA* is divergent from but contiguous with *cueR* (Fig. S2), which is the canonical arrangement for a *merR*-like operon. One exception was *Serratia marcescens*, in which *cueR* and *copA* are separated by a cluster of genes encoding for the biosynthesis of the antibiotic prodigiosin (*pigA-O*). Expression of *pig* genes is repressed by Cu but the physiological relevance of this observation is unclear (11). In agreement with a previous report, *ybaS* is also present

in nine additional genera from the *Enterobacteriacae* family, including *Edwardsiella* and *Yersinia*. However, consistent with its established function in acid tolerance, *ybaS* in these genomes is frequently encoded adjacent to *gadA/B* or *gadC* genes for AR (Fig. S3).

Cu stress in a Δ*copA* mutant is enhanced during growth in acidic conditions. To determine if there was a link between Cu and acid stress, we examined the inhibitory effects of added Cu on the growth of *E. coli* in minimal medium buffered at pH 5 and pH 7. Addition of up to 1.0 μM Cu did not impact growth of the wild type (WT) strain at either pH but it inhibited growth of the Δ*copA* mutant (Fig. 2). Notably, the amount of Cu required to completely suppress growth at pH 5 (0.1 μM, Fig. 2A) was less than the amount required at pH 7 (1.0 μM, Fig. 2B), suggesting that Cu stress in the Δ*copA* mutant was enhanced during growth in acidic conditions. The Cu-tolerant phenotype was restored upon expression of *copA via* plasmid-mediated complementation (Fig. 2). Identical results were obtained using the Δ*copA* mutants of other pathogenic and nonpathogenic strains of *E. coli* (Fig. S4), indicating that the interplay between Cu stress and acid stress is a conserved feature of *E. coli* physiology.

Addition of Cu to 0.05 μM was sufficient to affect growth at pH 5 and not at pH 7 (cf. Fig. S4, Fig. 2). However, this treatment led to a comparable rise in total intracellular Cu levels in mid-exponential Δ*copA* cells during growth at both pH values as determined by ICP MS (Fig. S5). Hence, the increase in Cu stress at pH 5 did not correlate with an increase in the amounts of trapped Cu. Nevertheless, Cu may become more bioavailable during growth at pH 5 due to protonation of thiols and amines, leading to a decrease in the Cu buffering capacity of the extracellular medium

or intracellular millieu. To report for bioavailable Cu, we used a *lacZ* transcriptional reporter fused to the *copA* promoter (P_{copA}-*lacZ*) (12). The latter is activated by CueR, the primary Cu sensor in *E. coli* (Fig. 1B). In agreement with a previous observation (13), background P_{copA}-*lacZ* activity in mid-exponential Δ*copA* cells was higher than in WT and it did not increase further in response to added Cu (Fig. S6A), suggesting that this mutant trapped trace amounts of Cu in its cytoplasm. Nevertheless, P_{copA}-*lacZ* activities in the Δ*copA* mutant were comparable irrespective of the pH of the culture medium (Fig. S6A). Similarly, the response of the P_{copA}-*lacZ* reporter to Cu was comparable in WT cultures grown at pH 5 and pH 7 (Fig. S6B). Thus, the present evidence did not support an increased cellular level or bioavailability of Cu at pH 5 under the experimental conditions employed here.

Exogenous Glu and Gln protect the Δ*copA* mutant from Cu stress at pH 5. Given the established role of *ybaS* in Gln-dependent acid tolerance, its demonstrated ability to contribute to Glu-dependent AR, and its synteny with *copA* and *cueR* (Fig. 1), we hypothesised that Cu stress during growth in acidic conditions is linked to Glu and/or Gln utilization. Indeed, addition of exogenous Glu and Gln (0.5 mM total) rescued the growth of the Δ*copA* mutant in Cu-supplemented medium at pH 5 (Fig. 3A) and pH 7 (Fig. 3B). This protection was also observed for other pathogenic and nonpathogenic strains of *E. coli* (Fig. S7). Compared with Gln, protection by Glu extended to higher Cu concentrations (Fig. S8).

Asp and Asn were also protective at pH 5 (Fig. S9A). In contrast, Arg, which is responsible for an alternative acid resistance system in *E. coli* (9), was only partially protective at pH 5 (Fig. S9B). Cys and the Cys-containing tripeptide glutathione were strongly protective (Fig. S9C), likely because these thiol-containing

molecules are high-affinity chelators of Cu. We also tested branched-chain amino acids (BCAAs, *ie.* Ile, Leu, and Val), which are known to rescue Cu-sensitive mutants of *E. coli* from Cu stress at pH 7 (13, 14). These amino acids rescued growth of the Δ*copA* mutant strongly at pH 7 (Fig. 3B) but only weakly at pH 5 (Fig. 3A), especially when compared with Glu and/or Gln. These results indicated that Cu stress at pH 5 led to a high requirement for exogenous Glu and/or Gln but not BCAAs. Nevertheless, addition of Glu and/or Gln did not restore Cu tolerance of the Δ*copA* mutant to WT levels. This observation and the varying protective effects of each amino acid are discussed below.

Cu stress leads to depletion in intracellular Glu concentrations. Glutamate is a key metabolite in *E. coli*, accounting for nearly 40% of all intracellular metabolites during exponential growth (15). The observed auxotrophy for Glu during Cu stress (Fig. 3) indicated that the internal pool of this amino acid was depleted. To test this hypothesis, *E. coli* was cultured with or without added Cu to the mid-logarithmic phase and the concentrations of free Glu in harvested cells were measured. As anticipated, growth in Cu-supplemented medium diminished the Glu pools in the Δ*copA* mutant (Fig. 4A). This effect was observed at both pH 5 (Fig. 4A(ii)) and pH 7 (Fig. 4A(i)) but less Cu was required at pH 5, consistent with our earlier finding that less Cu was required to inhibit the Δ*copA* mutant at pH 5 (Fig. 2). Intracellular Glu levels in WT cells remained unaffected under these conditions (Fig. 4A).

Our measurements further revealed that basal Glu levels in mid-exponential Δ*copA* cells cultured at pH 5 without any added Cu (~9 nmol Glu/mg protein, Fig. 4A(ii)) were lower than in cells cultured at pH 7 (~44 nmol Glu/mg protein, Fig.

4A(i)). This Glu-starved phenotype was likely associated with the consumption of this amino acid to maintain the internal pH during growth in mild acid, which could occur *via* the GadA/B decarboxylases (*cf.* Fig. 1B) (16, 17). Hence, the observed importance of exogenous Glu but not BCAAs or other amino acids during Cu stress at pH 5 (*cf.* Fig. 3A) may reflect the unique role for Glu for growth in acidic conditions.

Excess Cu inhibits Glu biosynthesis *via* glutamate synthase (GOGAT). Glutamate in *E. coli* is synthesized from α-ketoglutarate (α-KG), an intermediate in the TCA cycle, *via* two pathways (Fig. 4B). Glutamate dehydrogenase (GDH or GdhA) generates Glu from the reductive amination of α-KG. In the alternative pathway, condensation of Glu with ammonia by glutamine synthetase (GS or GlnA) yields Gln. Subsequent reductive transamination of Gln with α-KG by glutamate synthase (GOGAT or GltBD) generates two Glu molecules (a net gain of one). Together, GDH, GS, and GOGAT constitute the central pathway for nitrogen assimilation in *E. coli.* The GDH route is thought to be most efficient when ammonia is abundant, while GOGAT is important during ammonia limitation (18).

Addition of the Glu precursor α-KG failed to protect the Δ*copA* mutant from Cu stress at pH 5 and pH 7 (Fig. 3), implying that either GDH or GOGAT, or both, was inactive. Growth at pH 5 in the presence of added Cu did not reduce *gdhA* transcription (Fig. 4C(i)) or GDH activity (Fig. 4D(i)) in mid-exponential Δ*copA* cells. At pH 7, there was a decrease in *gdhA* transcription (Figures 4C(i)) but there was no loss in GDH activity (Fig. 4D(i)). By contrast, growth in Cu-supplemented medium at pH 5 reduced the activity of GOGAT in mid-exponential Δ*copA* cells by ca. 50% (Fig. 4D(ii)). GOGAT activity was also lost during growth in Cu-supplemented medium at pH 7 but the amount of Cu required to achieve this effect

was again higher than at pH 5 (Fig. 4D(ii)). There was no change in the levels of *gltB* transcription in these Cu-treated cultures (Fig. 4C(ii)), suggesting that Cu exerted an inhibitory effect at the protein level. Both GOGAT and GDH remained active in WT cells during growth at either pH, with or without added Cu (Fig. S10).

Cu-stressed Δ*copA* cultures displayed additional phenotypes consistent with GOGAT deficiency. There was a small but reproducible increase in GDH activity in Δ*copA* cells grown in Cu-rich medium at pH 5 (Fig. 4D(i)). Upregulation of GDH has been shown to compensate for the decrease in Glu biosynthesis in Δ*gltD* and Δ*gltB* mutant strains of *E. coli* and *Salmonella*, respectively (19). Decreasing the amount of ammonia in the culture medium further exacerbated Cu stress in Δ*copA* cells at both pH 7 and pH 5 (Fig. S11), consistent with GDH becoming more inefficient and increased reliance on GOGAT for making Glu (18) (*cf*. Fig. 4B).

Mechanism of GOGAT inhibition. GOGAT contains two [4Fe-4S] clusters in the active site. The decrease in GOGAT activity during Cu stress at pH 5 and pH 7 corresponded with reductions in the activities of two additional [4Fe-4S]-containing enzymes, namely NADH dehydrogenase I (NUO) and succinate dehydrogenase (SDH) (Fig. S12). These results suggested that Cu stress in our experimental conditions interfered with the synthesis, maturation, and incorporation of Fe-S clusters into enzymes *via* the Isc pathway as proposed previously (13, 14, 20). Yet, contrary to these prior reports, the amounts of Cu used in these experiments were not sufficient to induce expression of *sufA* and *sufB*, two genes that encode components of the Suf pathway for Fe-S cluster repair (Fig. S13A-B, discussed below).

Mature, solvent-accessible [4Fe-4S] clusters are also known to be destroyed by excess Cu (13, 21). To determine if GOGAT was poisoned directly by Cu, the

Δ*copA* mutant was cultured without any added Cu and, upon reaching mid-exponential phase, was exposed to added Cu (0–10 μM) for 30 min. Consistent with our hypothesis, this treatment had no effect on GDH activity but it reduced GOGAT activity in a dose-dependent manner (Fig. S14), suggesting that at least one of its [4Fe-4S] clusters is solvent-exposed. As a control, we confirmed that the activity of NUO remained unaffected (Fig. S14), likely because its [4Fe-4S] clusters are protected by the protein scaffold. However, the doses of Cu that poisoned GOGAT (~10 μM) were higher than doses that suppressed growth (< 1 μM, cf. Fig. 2, Fig. S4). Hence, we propose that the loss of GOGAT during Cu stress was associated primarily with the loss of [4Fe-4S] cluster biosynthesis (also see Supporting Discussion 1).

An implication for the loss of GOGAT at pH 5. The varying protective effects of amino acids during Cu stress as described earlier can be reconciled with an impaired GOGAT activity. Exogenous Glu was protective (Fig. 3) likely because it bypassed GOGAT and supplied cells with the final reaction product (*cf.* Fig. 4B). Similarly, Asp and Asn were protective (Fig. S9A) because these amino acids could act as substrates for an alternative route to Glu. The three enzymes involved in this pathway, aspartate aminotransferase (AspC) and the two asparaginases (AnsA and AnsB, Fig. S9A), are presumably Cu-tolerant because they do not require Fe-S clusters or other transition metal ions as cofactor.

As noted earlier, exogenous Glu did not restore Cu tolerance of the Δ*copA* mutant to WT levels, likely because multiple other Fe-S clusters were also inactivated (*eg.* NUO and SDH). While addition of Glu would alleviate the demand on GOGAT and upstream Fe-S enzymes that ultimately feed into the Glu pool (*eg.* aconitase), it would not relieve the block on other defective enzymes such as the Fe-S dehydratases

in the pathway for BCAA biosynthesis. Similarly, addition of BCAAs only partially rescued the Δ*copA* mutant from Cu stress (Fig. 3), likely because GOGAT and other Fe-S enzymes outside the BCAA biosynthesis pathway remained inactive.

It is important to highlight that at pH 5, the protective effect of BCAAs was diminished relative to Glu (Fig. 3A). This observation was consistent with the established requirement for Glu, but not BCAAs, for acid tolerance (*cf.* Fig. 1B). The K_m values for the two Glu decarboxylases in *E. coli* have been reported to range between 1 to 15 mM (22-24). Our estimate of the intracellular Glu pool at pH 5 was within this range (~9 nmol/mg protein or ~3 mM). Hence, we anticipate that the inability to synthesise Glu *via* GOGAT (and the corresponding decrease in the Glu pool) would impact the efficiency of acid tolerance under our experimental conditions.

Cu stress induces expression of YbaS and YbaT. Exogenous Gln was also protective, albeit to a lesser extent compared with Glu (Fig. S8). This observation was counterintuitive given that Gln is a co-substrate for GOGAT (Fig. 4B). However, like Asp and Asn, Gln can be converted to Glu independently from GOGAT by two separate glutaminases, namely YbaS (glutaminase A) and YneH (glutaminase B) (Fig. 4B). Although Cu stress did not affect YneH activity in mid-exponential Δ*copA* cells (Fig. 4D(iii)), it increased the activity of YbaS (Fig. 4D(iv)). This increase was observed during growth at pH 5 and pH 7, although again the amount of Cu required to achieve this effect was less at pH 5 (Fig. 4D(iv)). The upregulation in YbaS activity correlated with an increase in the levels of *ybaS* (Fig. 4C(iv)) and *ybaT* (Fig. S13C) expression. In contrast, expression of *yneH* was not altered in response to Cu (Fig. 4C(iii)).

In the simplest model, induction of *ybaST* in response to Cu stress would occur in a CueR-dependent manner (*cf.* Fig. 1). To test this hypothesis, we constructed a Δ*copA*Δ*cueR* double mutant. This mutant was reproducibly more Cu-sensitive than was the Δ*copA* parent strain at pH 5 (Fig. S15 and Supporting Discussion 2). Nevertheless, Cu treatment also increased the amounts of *ybaST* transcripts in the Δ*copA*Δ*cueR* mutant when compared with the untreated control (Fig. S16), suggesting that CueR did not directly regulate expression of *ybaST*, at least under our experimental conditions.

Although the *ybaS* and *ybaT* genes for acid tolerance were induced during Cu stress, the *copA* gene for Cu tolerance did not appear to be upregulated during acid stress. Basal expression levels of *copA* (Fig. S17) and activities of the P_{copA}-*lacZ* fusion (Fig. S6) in mid-exponential WT cells were comparable regardless of the growth pH. Thus, the evidence described in this work collectively point to an indirect and potentially complex relationship between Cu tolerance and acid tolerance systems.

The protective effect of Gln is suppressed in a Δ*ybaST* mutant. Our results led us to propose that YbaS and YbaT act as a compensatory pathway that offsets the loss in GOGAT and protects the intracellular Glu pool *via* hydrolysis of Gln and regeneration of Glu (Figs. 1B, 4B). The glutaminase activity of YbaS also produces ammonia, which contributes to overall acid tolerance (Fig. 1B) (7). This model predicts that the protective effect of exogenous Gln would be suppressed if YbaS and YbaT were inactive. To test this proposal, we mutated the entire *ybaST* operon in the Δ*copA* genetic background. The resulting Δ*copA*Δ*ybaST* mutant strain was confirmed to display no measurable YbaS activity (Fig. S18).

When cultured in the absence of added Gln, the Δ*copA*Δ*ybaST* mutant displayed a Cu-sensitive phenotype that was comparable to the Δ*copA* parent strain (Fig. S19). However, when the growth medium at pH 5 was supplemented with Gln (0.5 mM), the Δ*copA*Δ*ybaST* double mutant was demonstrably more Cu-sensitive than was the Δ*copA* parent strain, as evidenced by a prolonged lag phase in the presence of Cu (Fig. 5A). This observation indicated that the absence of functional *ybaS* and *ybaT* genes led to an increased sensitivity to Cu in the presence of Gln, or alternatively, a diminished protective effect of Gln during Cu stress. This phenotype was observed regardless of ammonia availability (Fig. S20). Expression of the *ybaST* operon on a plasmid fully restored YbaS activity (Fig. S18) and, subsequently, the protective effect of Gln (Fig. 5A). By contrast, deletion of *ybaST* had only a minor impact on Gln protection at pH 7, suggesting that this operon plays a less important role at pH 7 (Fig. 5B). These results confirmed that the protective effect of Gln against Cu stress during growth in acidic conditions required *ybaS* and *ybaT*, and they established a link between Cu stress, acid tolerance, and Gln utilisation.

DISCUSSION

The antibacterial activity of Cu is an important component of the mammalian innate immune defense (1). In response, bacterial pathogens mount a survival strategy that relies on the efflux of excess Cu ions from their cytoplasm. The *copA* genes of clinically significant pathogens, including *Mycobacterium tuberculosis* (3), *Streptococcus pneumoniae* (2), and *Klebsiella pneumoniae* (4), have been identified as a virulence factor in animal models of infection. We have previously described the synergistic action of Cu ions with other antibacterial agents that may be derived from

the host, such as nitric oxide (25) and hydrogen peroxide (26). Here we provide evidence that Cu ions and acid are also strong co-stressors.

Cu is a highly competitive metal that outcompetes weaker binding metals from sites in metalloproteins, leading to Cu intoxication in cells. Several proteins that contain Fe (particularly Fe-S clusters) (13, 14, 21, 26, 27), Zn (28), and Mn (29) have now been identified as targets of Cu poisoning. Since metalloproteins account for nearly half of all enzymes in cells (30), precisely which enzymes are mismetallated by Cu and the ensuing changes in bacterial physiology may vary, depending on the specific organism and experimental conditions. The latter do not always approximate the natural environment of the organism under investigation. In the case of *E. coli*, the unprecedented synteny of Cu tolerance genes with Gln-dependent acid tolerance genes in its chromosome may provide an insight. Importantly, this genetic arrangement is conserved in *E. coli*, implying strong selection pressure.

E. coli resides primarily in the lower intestines of mammals. During its interaction with the animal host, this bacterium experiences mild and extreme fluctuations in external pH in the stomach, intestinal lumen, genitourinary tract, and phagolysosomes of epithelial and innate immune cells. Recent evidence suggests that *E. coli* also encounters elevated levels of Cu in at least some of these sites. Survival of a Δ*copA* mutant within murine macrophages was impaired when compared with the WT (5). In uropathogenic *E. coli*, *copA*, as well as *cueO*, *cusC*, and *cusF* genes for Cu tolerance were highly expressed during human urinary tract infection, and this observation correlated with increased Cu concentrations in the urine of infected patients (31).

The combination of Cu and low pH poses a unique challenge to *E. coli* metabolism. Our *in vitro* work showed that excess Cu ions in the *E. coli* cytoplasm

may impair acid tolerance by disrupting Glu biosynthesis *via* GOGAT. However, our data also suggested that *E. coli* may use alternative enzymes, namely YbaS and YbaT, to overcome this block in Glu synthesis if exogenous Gln is supplied. Intriguingly, Gln is the most abundant amino acid in systemic circulation. Approximately 600 μM of free Gln is present in human blood plasma and nearly a third of this supply is turned over by gastrointestinal mucosa epithelial cells (32, 33). Gln is also indispensable for the proliferation and antimicrobial activity of innate immune cells (34). It is plausible that to survive *in vivo*, *E. coli* can alter its metabolism to access host Gln stores using the mechanisms identified in this work. Notably, both *ybaS* and *ybaT* were also upregulated along with *copA* during extraintestinal urinary tract infection in humans (31).

Other enteric bacteria, for example *Salmonella* and *Klebsiella*, share common colonisation routes and niches with *E. coli*, and they are presumably also exposed to the combination of acid and Cu stress. Like *E. coli*, both organisms use GOGAT to synthesise Glu. However, neither relies on Glu for acid tolerance (35) and thus poisoning of the Glu biosynthesis pathway would not have the same impact on their survival. It is worth noting that in these organisms, *copA* and *cueR* are contiguous, and homologues for YbaS and YbaT are absent (Fig. S2). The key targets of Cu stress in these organisms remain to be identified but for *Klebsiella pneumoniae*, [4Fe-4S] dehydratases in the pathway for branched-chain amino acid biosynthesis are major candidates, at least during colonisation of the lung (4).

How is *ybaST* upregulated by Cu? The intergenic region between *copA* and *ybaST* contains three regulatory sites (Fig. 1A): CueR, the primary Cu sensor in *E. coli* and regulator of *copA*; CpxR, which controls the global response to envelope stress; and GadX/W, which governs transcription of acid resistance genes including

gadA/B and *gadC*. MerR-like regulators regulate transcription of divergent sequences in both directions (36) but CueR does not appear to also control *ybaST* (Fig. S16). Meanwhile, the putative role of CpxR in *ybaST* transcription has not been experimentally tested (37). In contrast, regulation of *ybaST* by GadX and GadW is well established, and this occurs in a RpoS-dependent manner (38-40). Notably, RpoS and CpxR also contribute to the cellular adaptation to excess Cu (41, 42). Finally, our results link Cu stress to central nitrogen metabolism and thus additional control by the nitrogen response regulators, such as NtrB and NtrC, may be involved (18). These regulators sense intracellular Gln/Glu/α-KG ratios, which may shift during conditions of Cu stress (*cf.* Fig. 4A). Ntr regulation is further coupled with RpoS *via* the stringent response and the (p)ppGpp signaling alarmone (18, 43). It is likely that the *ybaST* operon is subject to a complex network of regulatory controls not unlike those identified for the *gadA/BC* genes for Glu-dependent AR. Further studies are required to elucidate how these hierarchies of regulation are coordinated.

Finally, we noted that Cu stress in our experimental conditions was sufficient to induce *ybaS* and *ybaT* but not the *suf* pathway for the repair of damaged iron-sulfur clusters (Fig. S13). Hence, we propose that upregulation of *ybaS* and *ybaT* represents subtle metabolic changes that may occur in the graded response to low physiological levels of Cu encountered in the host.

METHODS

Strains and culture conditions. *E. coli* EC958, UTI89, and MG1655 were used in this study as indicated. All strains were propagated from frozen glycerol stocks on antibiotic-free LB agar or, where specified, in liquid M9 medium. Strains carrying pSU2718 plasmids were propagated in the presence of chloramphenicol (30

μg/mL). Liquid cultures were prepared in modified M9 medium (3 g/L KH_2PO_4, 0.5 g/L NaCl, 1 mM $MgSO_4$, 0.1 mM $CaCl_2$, 16.5 μg/mL thiamine, 25 mg/mL nicotinamide) using glucose (1 g/L) as carbon source and ammonium chloride (1 g/L) as nitrogen source. The medium was buffered at pH 5 with Na-MES (50 mM) or at pH 7 with Na-MOPS (50 mM). These pH buffers do not form a stable complex with Cu^{2+} ions (44). The medium was used without any metal purification step. Cultures were inoculated to an initial OD_{600} of 0.01 and grown at 37 °C with shaking at 200 rpm.

Construction of mutants. Deletion mutants of *copA*, *cueR*, and the *ybaST* operon were constructed by λ-Red mediated homologous recombination using the *cat* or *kan* cassettes from plasmid pKD3 or pKD4, respectively, as the selection marker and primers listed in Table S1. The antibiotic marker was excised using a pCP20-Gm or pCP20-Amp plasmid encoding the FLP recombinase. Complemented mutants were generated by cloning the gene of interest into plasmid pSU2718 between *Bam*HI and *Xba*I cut sites and subsequent transformation.

Growth assays. Bacterial growth was monitored in U-bottomed 96-well microtitre plates using an automated microplate shaker and reader (FluoStar Optima, BMG Labtech). Each well contained 200 μL of culture supplemented with Cu and/or *L*-amino acids. Stocks of amino acids were prepared immediately before use. The microplate was sealed with a sterile gas-permeable polyurethane membrane (Sigma). OD_{600} values were recorded up to 16 h. Microplates were shaken at 200 rpm in the orbital mode between readings.

Biochemical analyses. Batch cultures (50 mL) were prepared in acid-washed glass flasks. Cu was added to the desired final concentration. Bacteria were cultured to the mid-exponential phase (OD_{600} ~ 0.3, ca. 4 doublings) and harvested by

centrifugation (4000 *g*, 4 ºC). The final pellets were processed further for the measurements of intracellular Glu contents, enzyme activities, and gene expression levels. Details are available in the SI Appendix.

Statistical analysis. All statistical analyses were performed using two-way ANOVA in GraphPad Prism7. Results were not corrected for multiple comparisons.

ACKNOWLEDGEMENT. We thank A. Turner (UQ) for critical reading of this paper, and R. Borthwick and attendees of the 10th International Biometals Symposium for insightful discussions.

REFERENCES

1. Djoko KY, Ong CL, Walker MJ, & McEwan AG (2015) The Role of Copper and Zinc Toxicity in Innate Immune Defense against Bacterial Pathogens. *J Biol Chem* 290(31):18954-18961.
2. Shafeeq S*, et al.* (2011) The cop operon is required for copper homeostasis and contributes to virulence in Streptococcus pneumoniae. *Mol. Microbiol.* 81(5):1255-1270.
3. Ward SK, Abomoelak B, Hoye EA, Steinberg H, & Talaat AM (2010) CtpV: a putative copper exporter required for full virulence of Mycobacterium tuberculosis. *Mol Microbiol* 77(5):1096-1110.
4. Bachman MA*, et al.* (2015) Genome-Wide Identification of Klebsiella pneumoniae Fitness Genes during Lung Infection. *mBio* 6(3):e00775.
5. White C, Lee J, Kambe T, Fritsche K, & Petris MJ (2009) A role for the ATP7A copper-transporting ATPase in macrophage bactericidal activity. *J. Biol. Chem.* 284(49):33949-33956.
6. Rensing C & Grass G (2003) *Escherichia coli* mechanisms of copper homeostasis in a changing environment. *FEMS Microbiol. Rev.* 27(2-3):197-213.
7. Lu P*, et al.* (2013) L-glutamine provides acid resistance for Escherichia coli through enzymatic release of ammonia. *Cell Res.* 23(5):635-644.
8. Brown G*, et al.* (2008) Functional and structural characterization of four glutaminases from Escherichia coli and Bacillus subtilis. *Biochemistry (Mosc.)* 47(21):5724-5735.
9. Richard H & Foster JW (2004) Escherichia coli glutamate- and arginine-dependent acid resistance systems increase internal pH and reverse transmembrane potential. *J Bacteriol* 186(18):6032-6041.
10. Moriel DG*, et al.* (2016) A Novel Protective Vaccine Antigen from the Core Escherichia coli Genome. *mSphere* 1(6).

11. Williamson NR, Simonsen HT, Harris AK, Leeper FJ, & Salmond GP (2006) Disruption of the copper efflux pump (CopA) of Serratia marcescens ATCC 274 pleiotropically affects copper sensitivity and production of the tripyrrole secondary metabolite, prodigiosin. *J. Ind. Microbiol. Biotechnol.* 33(2):151-158.
12. Djoko KY*, et al.* (2015) Copper(II)-Bis(Thiosemicarbazonato) Complexes as Antibacterial Agents: Insights into Their Mode of Action and Potential as Therapeutics. *Antimicrob. Agents Chemother.* 59(10):6444-6453.
13. Macomber L & Imlay JA (2009) The iron-sulfur clusters of dehydratases are primary intracellular targets of copper toxicity. *Proc. Natl. Acad. Sci. U. S. A.* 106(20):8344-8349.
14. Fung DKC, Lau WY, Chan WT, & Yan A (2013) Copper efflux is induced during anaerobic amino acid limitation in Escherichia coli to protect iron-sulfur cluster enzymes and its biogenesis. *J. Bacteriol.*
15. Bennett BD*, et al.* (2009) Absolute metabolite concentrations and implied enzyme active site occupancy in Escherichia coli. *Nat. Chem. Biol.* 5(8):593-599.
16. Moreau PL (2007) The lysine decarboxylase CadA protects Escherichia coli starved of phosphate against fermentation acids. *J Bacteriol* 189(6):2249-2261.
17. Roe AJ, McLaggan D, Davidson I, O'Byrne C, & Booth IR (1998) Perturbation of anion balance during inhibition of growth of Escherichia coli by weak acids. *J Bacteriol* 180(4):767-772.
18. van Heeswijk WC, Westerhoff HV, & Boogerd FC (2013) Nitrogen assimilation in Escherichia coli: putting molecular data into a systems perspective. *Microbiol. Mol. Biol. Rev.* 77(4):628-695.
19. Yan D (2007) Protection of the glutamate pool concentration in enteric bacteria. *Proc. Natl. Acad. Sci. U. S. A.* 104(22):9475-9480.
20. Tan G*, et al.* (2014) Copper binding in IscA inhibits iron-sulphur cluster assembly in Escherichia coli. *Mol Microbiol* 93(4):629-644.
21. Chillappagari S*, et al.* (2010) Copper stress affects iron homeostasis by destabilizing iron-sulfur cluster formation in Bacillus subtilis. *J. Bacteriol.* 192(10):2512-2524.
22. Fonda ML (1985) L-Glutamate decarboxylase from bacteria. *Methods Enzymol.* 113:11-16.
23. Tramonti A, De Biase D, Giartosio A, Bossa F, & John RA (1998) The roles of His-167 and His-275 in the reaction catalyzed by glutamate decarboxylase from Escherichia coli. *J Biol Chem* 273(4):1939-1945.
24. Thu Ho NA, Hou CY, Kim WH, & Kang TJ (2013) Expanding the active pH range of Escherichia coli glutamate decarboxylase by breaking the cooperativeness. *J Biosci Bioeng* 115(2):154-158.
25. Djoko KY*, et al.* (2012) Phenotypic characterization of a *copA* mutant of *Neisseria gonorrhoeae* identifies a link between copper and nitrosative stress. *Infect. Immun.* 80(3):1065-1071.
26. Djoko KY & McEwan AG (2013) Antimicrobial action of copper is amplified via inhibition of heme biosynthesis. *ACS Chem. Biol.* 8(10):2217-2223.
27. Azzouzi A*, et al.* (2013) Coproporphyrin III excretion identifies the anaerobic coproporphyrinogen III oxidase HemN as a copper target in the Cu -ATPase mutant copA of Rubrivivax gelatinosus. *Mol. Microbiol.*

28. Tottey S*, et al.* (2012) Cyanobacterial metallochaperone inhibits deleterious side reactions of copper. *Proc. Natl. Acad. Sci. U. S. A.* 109(1):95-100.
29. Johnson MD, Kehl-Fie TE, & Rosch JW (2015) Copper intoxication inhibits aerobic nucleotide synthesis in Streptococcus pneumoniae. *Metallomics* 7(5):786-794.
30. Andreini C, Bertini I, Cavallaro G, Holliday GL, & Thornton JM (2008) Metal ions in biological catalysis: from enzyme databases to general principles. *J. Biol. Inorg. Chem.* 13(8):1205-1218.
31. Subashchandrabose S*, et al.* (2014) Host-specific induction of Escherichia coli fitness genes during human urinary tract infection. *Proc. Natl. Acad. Sci. U. S. A.* 111(51):18327-18332.
32. Stein WH & Moore S (1954) The free amino acids of human blood plasma. *J Biol Chem* 211(2):915-926.
33. Windmueller HG & Spaeth AE (1974) Uptake and metabolism of plasma glutamine by the small intestine. *J Biol Chem* 249(16):5070-5079.
34. Newsholme P (2001) Why is L-glutamine metabolism important to cells of the immune system in health, postinjury, surgery or infection? *J. Nutr.* 131(9 Suppl):2515S-2522S; discussion 2523S-2514S.
35. McClelland M*, et al.* (2000) Comparison of the Escherichia coli K-12 genome with sampled genomes of a Klebsiella pneumoniae and three salmonella enterica serovars, Typhimurium, Typhi and Paratyphi. *Nucleic Acids Res.* 28(24):4974-4986.
36. Lund PA, Ford SJ, & Brown NL (1986) Transcriptional regulation of the mercury-resistance genes of transposon Tn501. *J. Gen. Microbiol.* 132(2):465-480.
37. De Wulf P, McGuire AM, Liu X, & Lin EC (2002) Genome-wide profiling of promoter recognition by the two-component response regulator CpxR-P in Escherichia coli. *J Biol Chem* 277(29):26652-26661.
38. Tramonti A, De Canio M, & De Biase D (2008) GadX/GadW-dependent regulation of the Escherichia coli acid fitness island: transcriptional control at the gadY-gadW divergent promoters and identification of four novel 42 bp GadX/GadW-specific binding sites. *Mol Microbiol* 70(4):965-982.
39. Tucker DL*, et al.* (2003) Genes of the GadX-GadW regulon in Escherichia coli. *J Bacteriol* 185(10):3190-3201.
40. Seo SW, Kim D, O'Brien EJ, Szubin R, & Palsson BO (2015) Decoding genome-wide GadEWX-transcriptional regulatory networks reveals multifaceted cellular responses to acid stress in Escherichia coli. *Nat. Commun.* 6:7970.
41. Macomber L, Rensing C, & Imlay JA (2007) Intracellular copper does not catalyze the formation of oxidative DNA damage in Escherichia coli. *J Bacteriol* 189(5):1616-1626.
42. Yamamoto K & Ishihama A (2005) Transcriptional response of Escherichia coli to external copper. *Mol Microbiol* 56(1):215-227.
43. Brown DR, Barton G, Pan Z, Buck M, & Wigneshweraraj S (2014) Nitrogen stress response and stringent response are coupled in Escherichia coli. *Nat. Commun.* 5:4115.
44. Mash HE, Chin YP, Sigg L, Hari R, & Xue H (2003) Complexation of copper by zwitterionic aminosulfonic (good) buffers. *Anal. Chem.* 75(3):671-677.

1

FIGURES

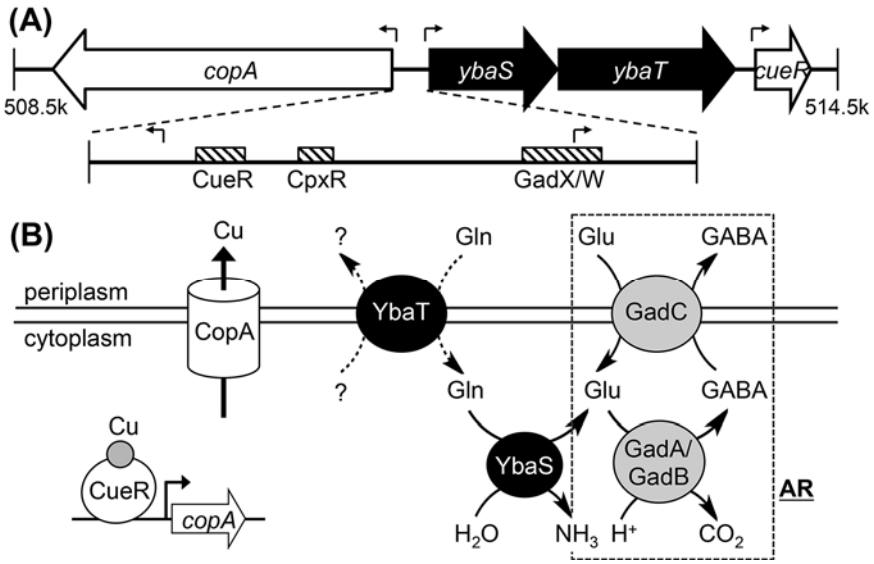

Figure 1. Clustering of Cu tolerance and acid tolerance genes in *E. coli*. (A) Genomic context of *copA* and *cueR* in *E. coli*. Figure shows the approximate locations of genes on the reference genome (RefSeq NC_000913.3). Block arrows represent directions of open reading frames. Transcription start sites are indicated by bent line arrows. Striped boxes represent binding sites for transcription factors (CueR, accttccagcaaggggaaggt; CpxR, gtaaaagtccgtaaa; GadX/W, taaatcaggatgcctgaaaatcggcaccgggggtg). **(B) Biochemical function of CopA, CueR, YbaS, and YbaT.** CueR is a Cu sensor while CopA is a Cu efflux pump. Both constitute the central mechanism for Cu tolerance in *E. coli*. YbaS is a glutaminase while YbaT is a putative Gln-importing permease. The dashed box shows components of the Glu-dependent acid resistance system (AR), namely the glutamate decarboxylases GadA and GadB, as well as the Glu/GABA-antiporter GadC. Both YbaS and YbaT are thought to support the function of this AR.

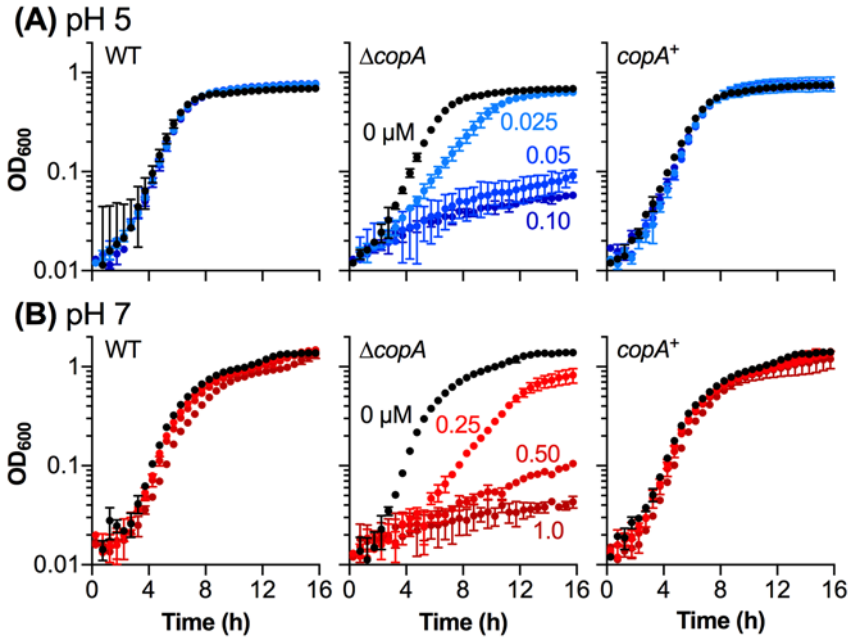

Figure 2. Cu stress during growth under different pH conditions. Growth of *E. coli* EC958 WT, Δ*copA* mutant, and *copA*$^{+}$ complemented mutant: **(A)** at pH 5 in the presence of 0 – 0.10 μM added Cu and **(B)** at pH 7 in the presence of 0 – 1.0 μM added Cu. Data were averaged from three independent experiments. Error bars represent ± SD.

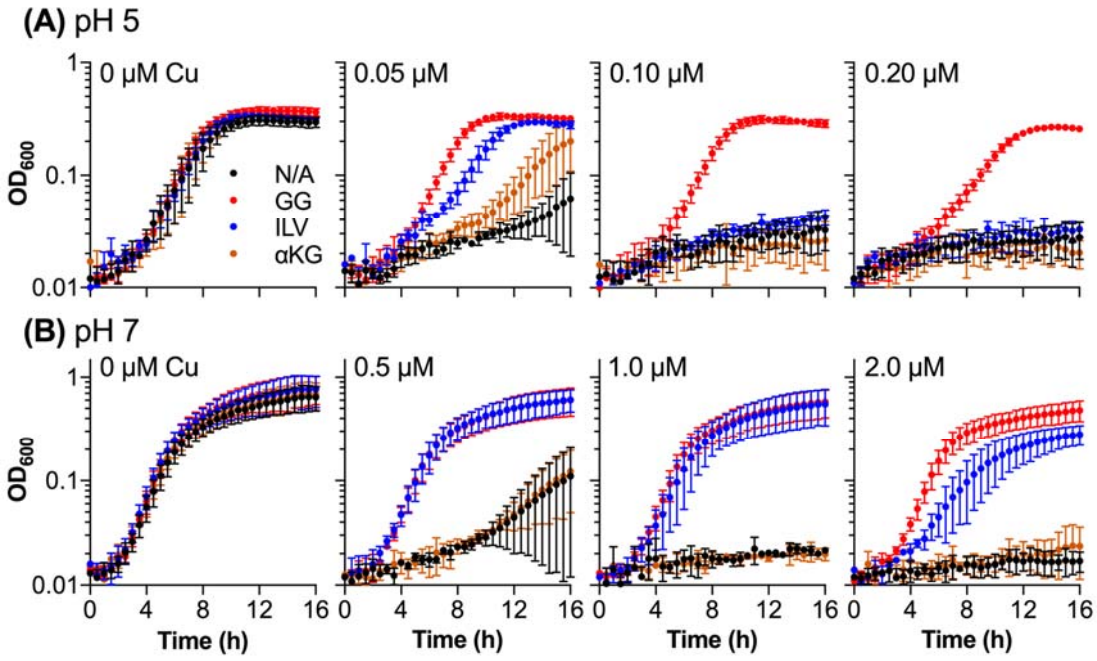

Figure 3. Protective effects of Glu and Gln. *E. coli* UTI89 Δ*copA* mutant was cultured **(A)** at pH 5 in the presence of 0 – 0.2 μM added Cu or **(B)** at pH 7 in the presence of 0 – 2.0 μM added Cu. The medium was supplemented with water (black, N/A); Glu and Gln (red, GG); Ile, Leu, and Val (blue, ILV); or α-ketoglutarate (orange, αKG). The total concentration of amino acids in each experiment was 0.5 mM. Data were averaged from three independent experiments. Error bars represent ± SD.

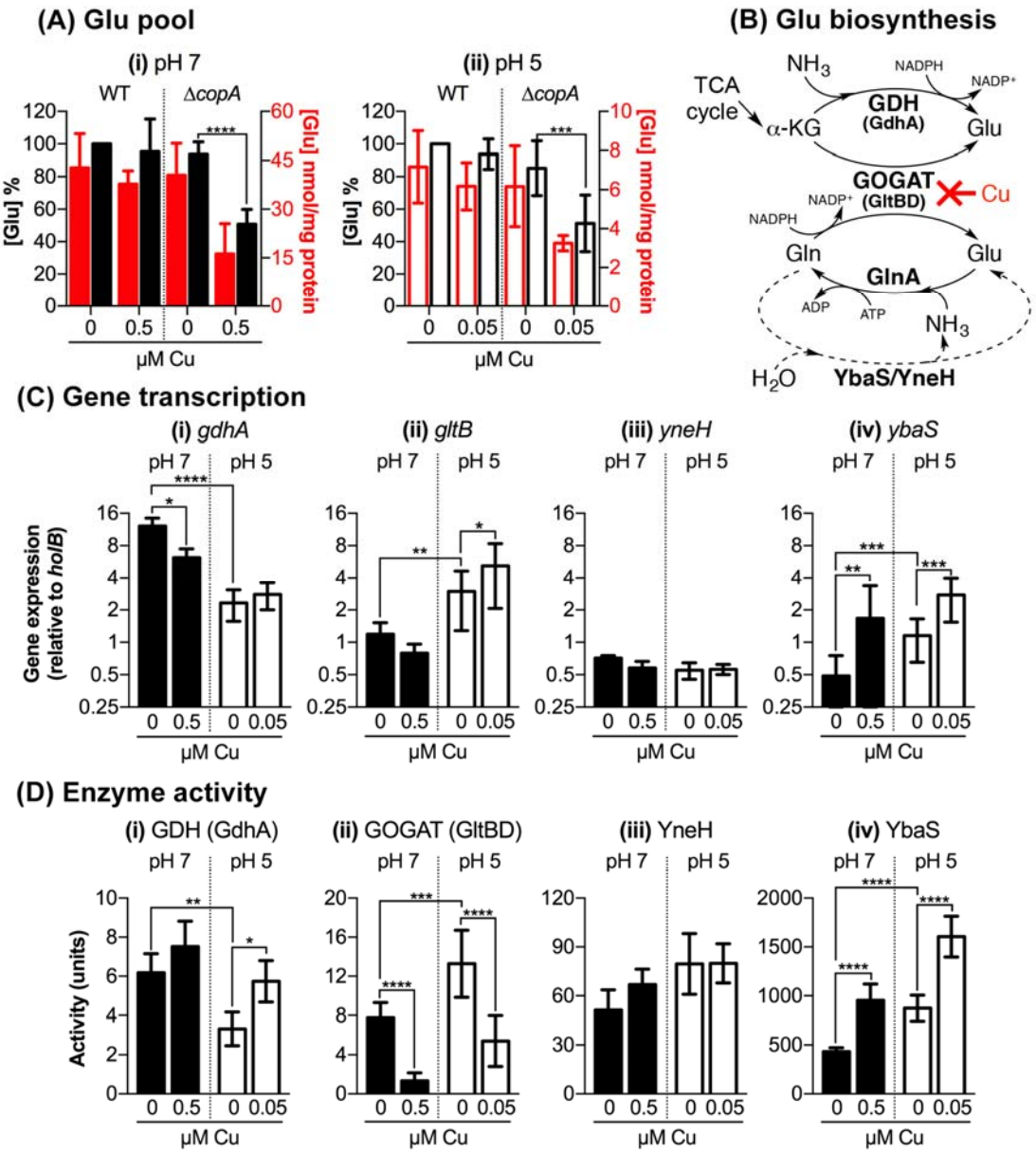

Figure 4. Effects of Cu on glutamate biosynthesis in *E. coli*. (A) Intracellular Glu concentrations. *E. coli* UTI89 WT and Δ*copA* mutant were cultured at **(i)** pH 7 or **(ii)** pH 5 with or without added Cu as indicated. Intracellular concentrations of Glu were shown as absolute values (red columns) or as a percentage relative to untreated WT (black columns). Data were averaged from five independent biological replicates. **(B) Glu biosynthesis pathways.** *De novo* synthesis of Glu begins with α-KG from the TCA cycle. This process is catalysed either by GDH using ammonia as the nitrogen donor (top pathway) or by GOGAT using Gln as the nitrogen donor (middle

pathway). Glu can also be generated by the hydrolysis of Gln. This process is catalysed by YbaS or YneH (bottom pathway). Our data show that excess Cu inhibits biosynthesis at the GOGAT step. The figure also shows one route of Glu consumption *via* GS, which also generates Gln. **(C) Activities of Glu biosynthesis genes.** The Δ*copA* mutant was cultured at pH 7 (black columns) or pH 5 (white columns) with or without added Cu as indicated. Activities of **(i)** GDH, **(ii)** GOGAT, **(iii)** YneH, and **(iv)** YbaS were measured in cell-free lysis extracts. Data were averaged from six independent biological replicates. **(D) Activities of Glu-synthesizing enzymes.** The Δ*copA* mutant was cultured at pH 7 (black columns) or pH 5 (white columns) with or without added Cu as indicated. Amounts of **(i)** *gdhA*, **(ii)** *gltB*, **(iii)** *yneH*, and **(iv)** *ybaS* transcripts relative to *holB* were measured by qPCR. Data were averaged from six independent biological replicates. **(A), (C), and (D)** Error bars represent ± SD. $^{****}P < 0.0001$, $^{***}P < 0.001$, $^{**}P < 0.01$, $^{*}P < 0.05$.

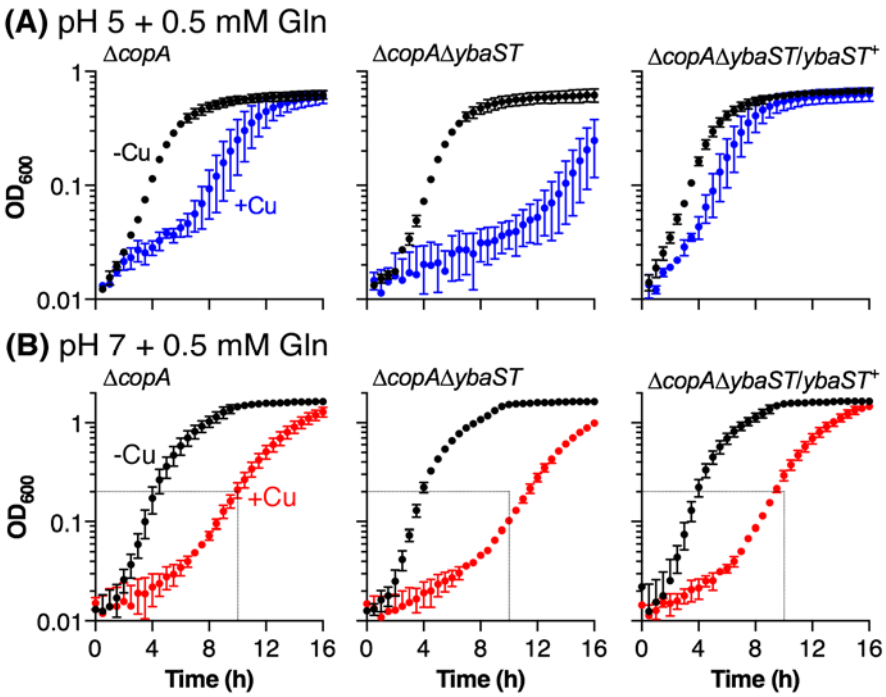

Figure 5. Effects of Δ*ybaST* mutation on Gln-dependent Cu tolerance. *E. coli* EC958 Δ*copA* mutant, Δ*copA*Δ*ybaST* double mutant, and Δ*copA*Δ*ybaST*/*ybaST*$^{+}$ complemented mutant were cultured **(A)** at pH 5 in the presence of 0 (black, -Cu) or 0.05 (blue, +Cu) µM added Cu or **(B)** at pH 7 in the presence of 0 (black, -Cu) or 0.5 (red, +Cu) µM added Cu. The medium was supplemented with 0.5 mM Gln. The inoculum, used in each experiment was pre-cultured in the same pH. Data were averaged from three independent experiments. Error bars represent ± SD.

SI APPENDIX

Interplay between tolerance mechanisms to copper and acid stress in *Escherichia coli*

Karrera Y. Djoko*, Minh-Duy Phan, Kate M. Peters, Mark J. Walker, Mark A. Schembri, and Alastair G. McEwan

School of Chemistry and Molecular Biosciences and Australian Infectious Diseases Research Centre, The University of Queensland, St Lucia, QLD 4072, Australia

SI Discussion 1.

Fig. S14 suggested that the amount of Cu required to directly inhibit the activity of mature GOGAT enzyme was higher at pH 5 (10 μM *vs.* 1 μM at pH 7). Earlier, we showed that expression of *gltB* was higher at pH 5 (Fig. 4C(ii)). Similarly, GOGAT activities were higher at pH 5 (Fig. 4D(ii), Figure S10). Therefore, the intracellular concentration of GOGAT enzyme was likely higher in cells cultured at pH 5. Consistently, a higher amount of Cu was required to inhibit GOGAT activity directly at pH 5.

These results seemed to contradict results in Fig. 4D(ii), in which lower amounts of Cu were required to achieve inhibition of GOGAT during growth at pH 5 (0.05 μM *vs.* 0.5 μM at pH 7). However, in these earlier experiments, Cu was added to the culture at the start of the growth and GOGAT activity was measured only when cells reached the mid-exponential phase (after at least 4 generations). The observed loss in GOGAT activity here would be the combined effect of direct enzyme inactivation (as shown in Fig. S14) as well as inhibition of downstream processes that may affect enzyme biogenesis, *eg. via* the Isc pathway for Fe-S cluster assembly (as shown Fig. S12).

SI Discussion 2.

The Δ*copA*Δ*cueR* mutant was found to be reproducibly more Cu-tolerant at pH 7 compared with the Δ*copA* parent strain when growth was assessed in parallel (Fig. S15). The mechanism for the increased tolerance at pH 7 is unknown and is beyond the scope of our work.

At pH 5, the Δ*copA*Δ*cueR* double mutant was reproducibly more Cu-sensitive than was the Δ*copA* parent strain (Fig. S15). On several occasions, growth of the Δ*copA*Δ*cueR* mutant was affected even in the absence of added Cu and background expression levels of *ybaS* and *ybaT* genes were higher than usual. This was likely a consequence of trace Cu in the

culture medium, which varied between 10–20 nM. These basal amounts of Cu approached inhibitory levels and the precise threshold varied with medium preparations.

To determine if Cu stress induced the expression of *ybaS* and *ybaT* in the Δ*copA*Δ*cueR* mutant, we cultured this mutant in the presence of 30 nM Cu. Parallel experimentation with the the Δ*copA* mutant (in the same media preparation, in the presence of 50 nM Cu as usual) as a positive control yielded consistent results and *ybaS* and *ybaT* were reproducibly upregulated during Cu stress (Fig. S16). However, given the challenges described above, it was difficult to obtain reproducible results with the Δ*copA*Δ*cueR* mutant. On the basis that we were able to find three independent replicates where *ybaS* and *ybaT* were upregulated by Cu (Fig. S16), we concluded that CueR does not control *ybaS* and *ybaT* directly under our experimental conditions.

SI Methods

Bioinformatic analyses. The nucleotide sequences of the *copA-ybaST-cueR* locus from *E. coli* K-12 str. MG1655 (6526 bp, RefSeq NC_000913.3) and the *copA-cueR* locus from *S. enterica* subsp. *enterica* sv. Typhimurium str. LT2 (3029 bp, RefSeq NC_003197.1) were used to query all complete genomes on NCBI (5975 available, last accessed 24/11/2016) using MegaBLAST (v.2.4.0+). Results were visualized using ggplot2 (v.2.2.0) in R (v.3.3.1). Distribution of YbaS was determined by tblastn against the same database with a threshold of 60% identity and 80% coverage. Genomic context was illustrated using Easyfig (1) with manual modification using Inkscape (v.0.91).

Measurement of intracellular Glu content. Bacterial pellets from batch cultures (50 mL) were resuspended in MeOH/MeCN/H_2O (40/40/20 v/v/v %) with frequent vortexing and re-centrifuged. The supernatant was evaporated to dryness under vacuum at 40 ºC and the

resulting pellet was resuspended in water. Insoluble debris were removed by centrifugation and the supernatant was added to a reaction mixture containing hydrazine (250 mM), ADP (1 mM), NAD^+ (1.6 mM), and *L*-glutamic dehydrogenase (Sigma G7882, 160 µg/mL) in Tris-Cl buffer (100 mM, pH 9). The mixture was incubated at 37 ºC for 30–60 min. Glu concentrations in the samples were estimated by comparing final absorbance values at 340 nm against a standard curve. Glu levels in UTI89 strains cultured at pH 7 and pH 5 were routinely measured to be ~44 and ~9 nmol/mg protein, respectively. A parallel culture in Gutnick medium (2) without any added Cu yielded ~90 nmol Glu/mg protein, suggesting that our culture conditions in modified M9 medium were Glu-limiting, particularly at pH 5.

Measurements of enzyme activities. Centrifuged bacterial pellets from batch cultures (50 mL) were resuspended in 0.5 mL of Na-HEPES buffer (50 mM, pH 7.4) and lysed by sonication (5 × 10 s bursts,10 W each). Each lysate was centrifuged and the supernatant was added into the appropriate reaction mixture in Na-HEPES buffer (50 mM, pH 7.4) as described below. All reactions were performed at 37 ºC. Amounts of proteins in samples were quantified using QuantiPro™ BCA Assay Kit (Sigma).

GOGAT and GDH activities were determined by following the oxidation of NADPH (0.25 mM). Gln (2.5 mM) and □-KG (2.5 mM) were used as substrates for GOGAT. Absorbance values at 340 nm were monitored continuously for 2 min (1 U = 10 nmol NADPH oxidised/min/µg protein). Gln was replaced with ammonium chloride (25 mM) for GDH (1 U = 1 nmol NADPH oxidised/min/µg protein). The activity of NUO was estimated by following the oxidation of deamino-NADH (Sigma N6756, 0.25 mM) at 340 nm for 2 min (1 U = 1 nmol deamino-NADH oxidised/min/mg protein). SDH activity was determined by monitoring the reduction of thiazolyl blue tetrazolium bromide (MTT, 0.15 mM) at 570 nm for 15 min in the presence of sodium succinate (5 mM) and phenazine methosulfate (PMS,

0.5 mM) (1 U = 1 nmol of MTT reduced/min/mg protein). To estimate the activities of YbaS and YneH, cell-free lysate supernatants were incubated with Gln (50 mM) at 37 ºC for 20 min in MES (100 mM, pH 5.5) and HEPES (100 mM, pH 7.4) buffer, respectively. The mixture was heated to 75 ºC for 5 min to deactivate all enzymes and chilled to 4 ºC. Enzyme activities were estimated from the amount of Glu generated in the reaction (1 U = 1 nmol Glu hydrolysed/min/mg protein).

RNA extraction and measurement of gene transcripts. For RNA extraction, 1 mL of the batch culture was harvested separately by centrifugation (15,000 *g*), snap-frozen, and stored at −80 ºC until further use. Bacterial RNA was extracted using the RNeasy Mini Kit (QIAGEN) and treated with DNAseI using the RNase-Free DNase Set (QIAGEN). cDNA was generated from 0.5 µg of RNA using the SuperScript® III First-Strand Synthesis System (Invitrogen). qPCR analyses were performed in 10 µL reactions using 2 ng of cDNA as template and 0.4 µM of the appropriate primer pairs (Table S2). Each sample was analysed in three technical replicates. Amplicons were detected with SYBR Green 2 in a QuantStudio 6 Flex Real-Time PCR System (Applied Biosystems). C_q values were calculated using LinRegPCR (3) after correcting for amplicon efficiency. *holB*, which encodes for DNA polymerase III, was used as the reference gene as its expression was not affected by metal ions (4).

SI References

1. Sullivan MJ, Petty NK, & Beatson SA (2011) Easyfig: a genome comparison visualizer. *Bioinformatics* 27(7):1009-1010.

2. Bennett BD*, et al.* (2009) Absolute metabolite concentrations and implied enzyme active site occupancy in Escherichia coli. *Nat. Chem. Biol.* 5(8):593-599.

3. Ramakers C, Ruijter JM, Deprez RH, & Moorman AF (2003) Assumption-free analysis of quantitative real-time polymerase chain reaction (PCR) data. *Neurosci. Lett.* 339(1):62-66.

4. Graham AI*, et al.* (2009) Severe zinc depletion of Escherichia coli: roles for high affinity zinc binding by ZinT, zinc transport and zinc-independent proteins. *J Biol Chem* 284(27):18377-18389.

SI TABLES

Table S1. Primers used for making mutant strains. All primers were purchased from Integrated DNA Technologies (Australia). Sequences belonging to the *cat* and *kan* cassettes from pKD3 and pKD4 plasmid, respectively, are in lowercase. Sequences belonging to *E. coli* strain UTI89 (RefSeq NC_007946.1) or EC958 (RefSeq NZ_HG941718.1) are in UPPERCASE. Restriction sites are in **bold**. Ribosomal binding sites are underlined.

Target	Flanking region	Primer Name	Sequence (5' → 3')
	5'	F	CTTTGTCCTGTACCGCCTGC
		R	ggaataggaactaaggaggaGGTCAGGTCGATAGTTTGTG
	3'	F	cctacacaatcgctcaagacGTGAGTAACGCCAACCGCTT
		R	AAATGGGTTAATGGCAAGGC
	5'	F	CCTCAGAAACCGCTGTCAGT
		R	ggaataggaactaaggaggaTTTGTTTGCATCTAACATCTTTTGT
	3'	F	cctacacaatcgctcaagacATGAAGCGCAATAAAACCGTATAAC
		R	TTTTCGATAATCGGGCAGTC
	5'	F	AAATGGGTTAATGGCAAGGC
		R	ggaataggaactaaggaggaGTGAGTAACGCCAACCGCTT
	3'	F	cctacacaatcgctcaagacATGAAGCGCAATAAAACCGTATAAC
		R	TTTTCGATAATCGGGCAGTC
	5'	F	TCATGGACAACATGGGCAGC
		R	gaagcagctccagcctacacaTCGCTAATGTTCATCGTTCG
	3'	F	ctaaggaggatattcatatgCTCTCCGGCTGCTGTCAT
		R	ACAGCGTCAGACGGCTATTT
pSU2718 *-copA*	-	F	*catgga***GGATCC**ttaaagaggagaaaggtaccgcATGTCACAAACTATCGACCTGAC
		R	*ttacgc***TCTAGA**CGCATCCGCAATGATGTACT
pSU2718 *-ybaST*	-	F	*catgga***GGATCC**ttaaagaggagaaaggtaccgcATGTTAGATGCAAACAAATTACAGC
		R	*ttacg***CTCTAGA**TGTGCTTTGTTAAAGGGTTTCA

[a]These primers were used to generate the Δ*copA* mutant in both UTI89 and EC958 backgrounds.
[b]This mutation was introduced in the UTI89Δ*copA* background to generate UTI89Δ*copA*Δ*cueR* double mutant.

Table S2. Primers used for analyses of gene transcription by qPCR. Primers were purchased from Sigma (Australia). Genome sequence of *E. coli* strain UTI89 (RefSeq NC_007946.1) was used as template.

Amplicon name	Primer sequence (5' → 3')	Amplicon length (bp)
copA	F: ATGACGATGACAGCCAGCAG R: TTTACCCGTGCCTGAGTGAC	112
cueO	F: AACCAGTGAAGGTGAGCGAG R: CATCCCCATCTGACTGACCG	119
cueR	F: GAAGAGAAGGGGCTGGTGAC R: CCTCCAGGTTAAAGCCCACC	124
gltB	F: AAGGTCTGTGTATGCCGACG R: GCGGTACGGTGTTAGTGGAG	114
holB	F: GTGGTGCGAAAGTTGTCTGG R: CGCGGGTAGCAAGGAAAAAC	120
sufA	F: GCTTTGGCTATGTGCTCGAC R: CTTGCAGCGGGACAAACAG	93
sufB	F: TGGAGATGGAAGAACCGCAC R: GTCACAATTACCGCACGATGG	98
ybaS	F: ACCAACTTCCATAACCGGGC R: TTGATGAGCGTGGAGCACTG	113
ybaT	F: TAAGCAACCATGCGGTAGGG R: AGAAACGGAAATATGCGCCG	119

SUPPORTING FIGURES

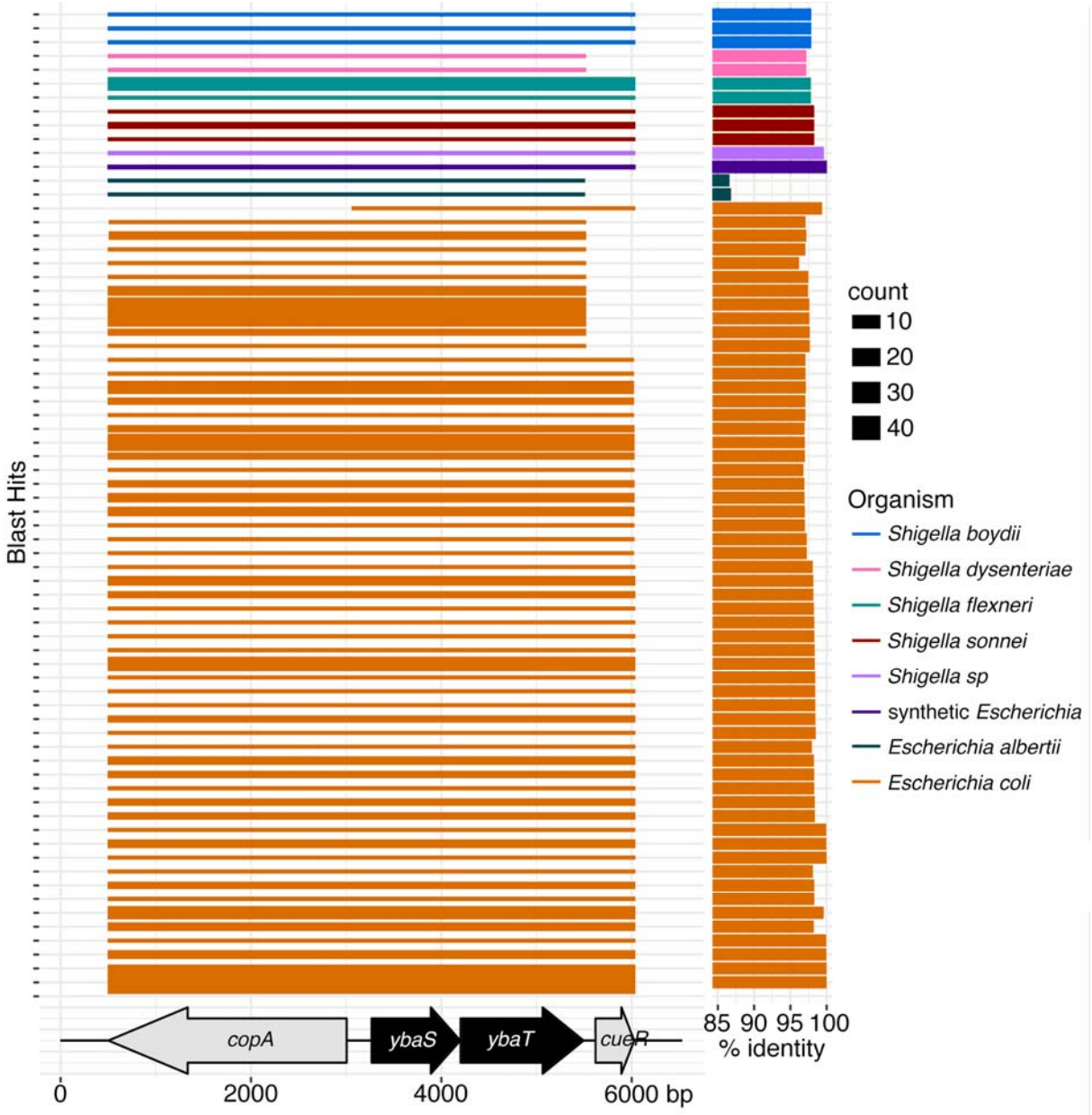

Figure S1. Sequence alignments of *copA-ybaST-cueR* loci. The sequence of the *copA-ybaST-cueR* locus from *E. coli* was used as a query in a BLASTn search against 5975 complete bacterial genomes. The search yielded a total of 232 positive hits with alignment length covering *ybaST*. Each horizontal line represents a unique alignment group belonging to the same species that has the same % identity over the same alignment length. The line thickness represents the number of hits in each group and is coloured according to species name.

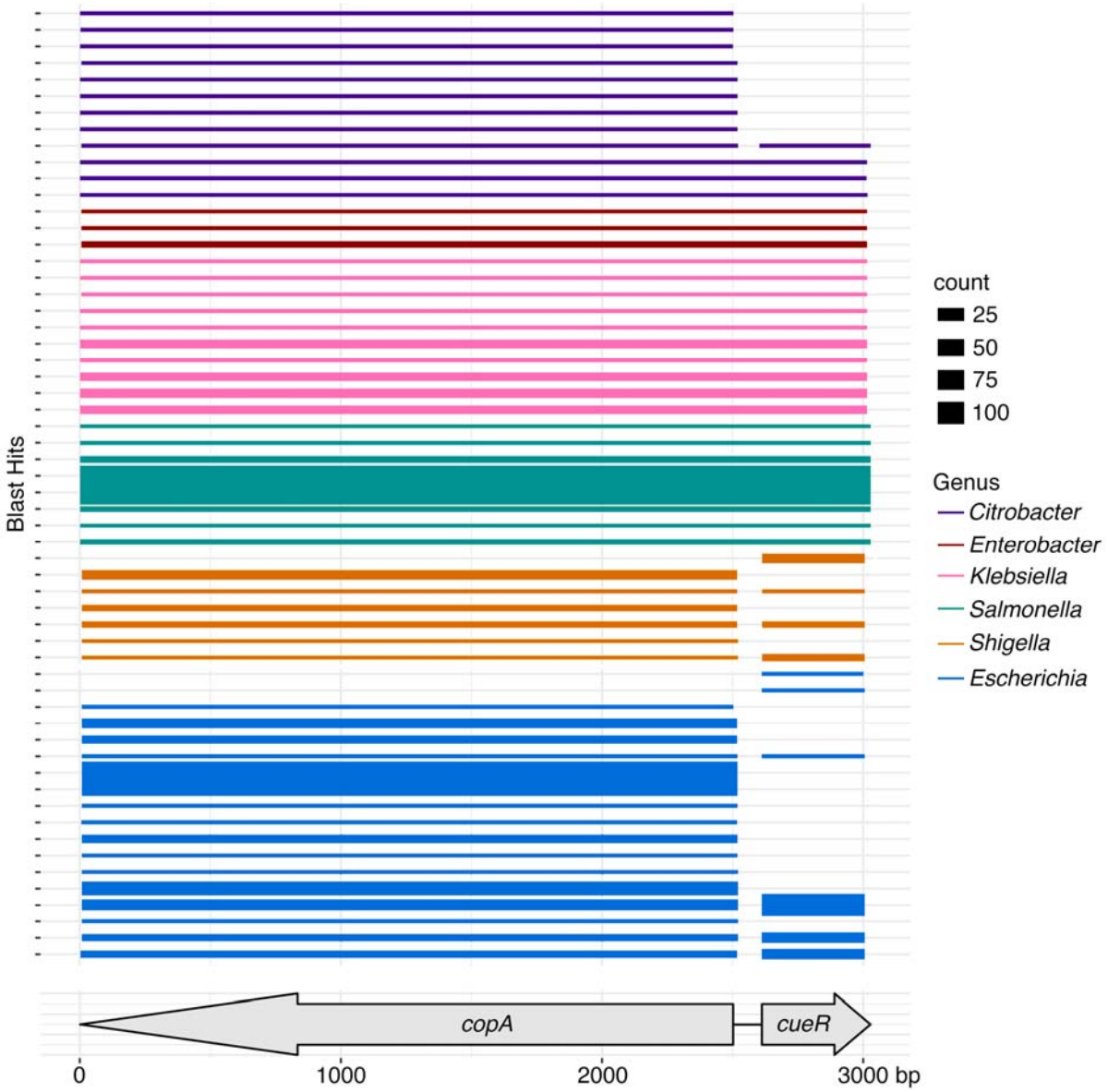

Figure S2. Sequence alignments of *copA-cueR* loci. The sequence of the *copA-cueR* locus from *S. enterica* sv. Typhimurium was used as a query in a BLASTn search against 5975 complete bacterial genomes. The search yielded a total of 262 positive hits with alignment length covering *copA* and *cueR* without *ybaST* insertion, shown by continuous horizontal lines with no gap. Hits from *Escherichia* and *Shigella* genera, which include *ybaST* insertion were also shown by horizontal lines with a gap between *copA* and *cueR* for comparison. Each horizontal line represents a unique alignment group belonging to the same species that has the same % identity over the same alignment length. The line thickness represents the number of hits in each group and is coloured according to species name.

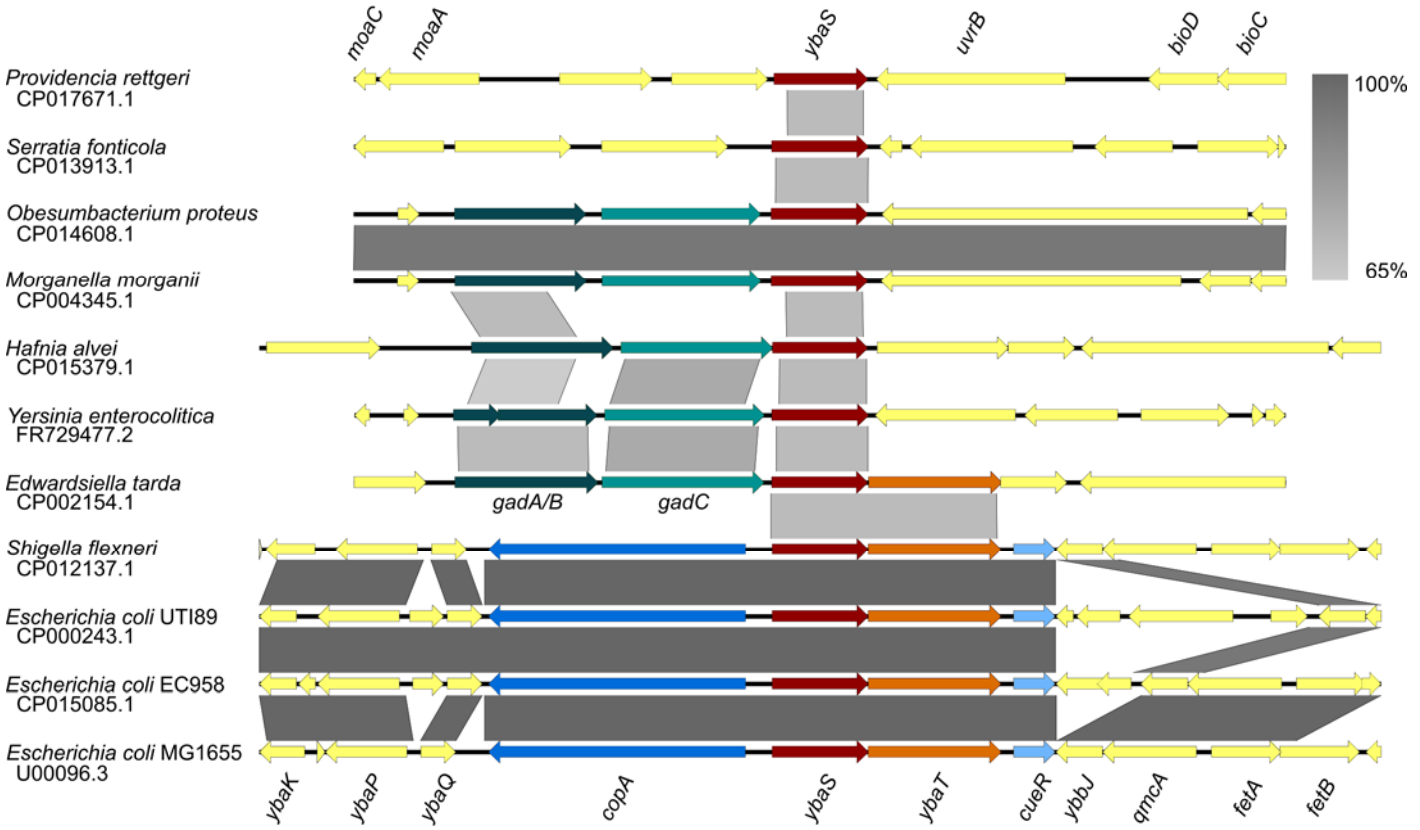

Figure S3. Genomic context of *ybaS* in several *Enterobactericeae* species. The protein sequence of YbaS was used to query 5975 complete bacterial genomes by tblastn. The search identified 325 genomes positive for YbaS (>60% identity over 80% coverage) from 15 genera. One genome per genus from *Enterobacteriaceae* family was chosen to represent the YbaS-encoding locus plus 5 kb flanking regions. The *copA-ybaS-ybaT-cueR* arrangement is confined within *E. coli* and *Shigella* while *ybaS* is located elsewhere in the genomes of other genera.

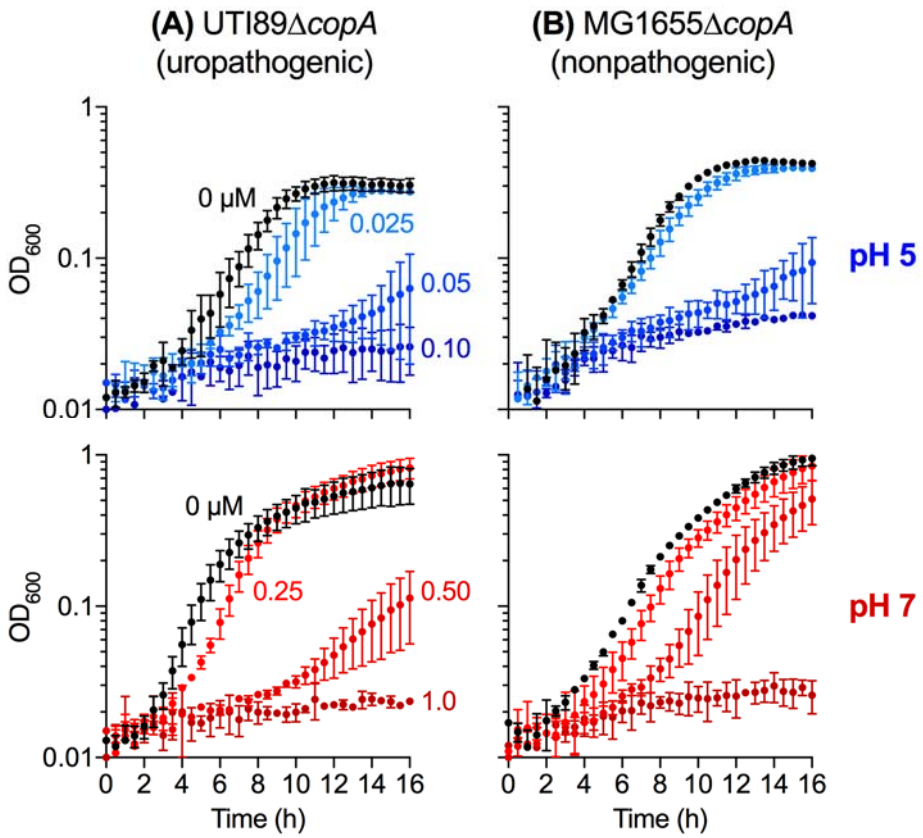

Figure S4. Cu stress in different *E. coli* strains. The Δ*copA* mutant strains of **(A)** UTI89 and **(B)** K-12 substr. MG1655 were cultured at pH 5 and pH 7 in the presence of various concentrations of Cu as indicated. Data were averaged from three independent experiments. Error bars represent ± SD.

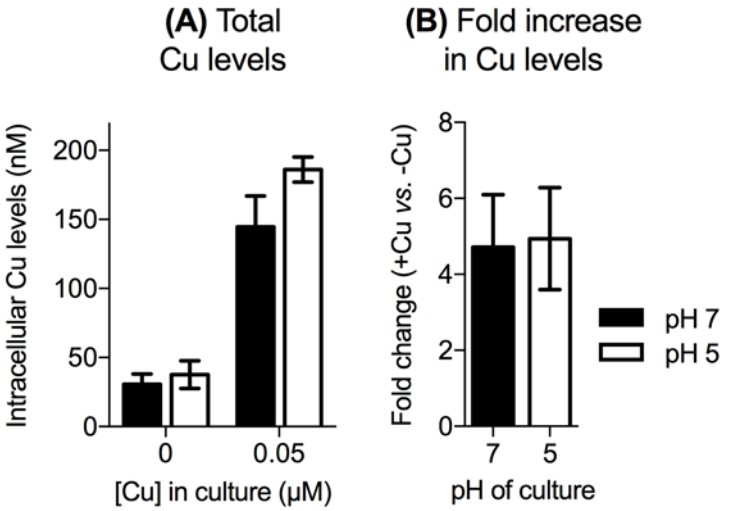

Figure S5. (A) Total amounts of intracellular Cu in UTI89Δ*copA*. Bacteria were cultured at pH 7 (black columns) or pH 5 (white columns) to a final OD_{600} of ~0.3. The medium was supplemented with 0 or 0.05 μM Cu as indicated. Bacteria were centrifuged, washed once with ice-cold PBS containing 1 mM EDTA and twice more with ice-cold PBS without any EDTA. Bacterial pellets were dried overnight at 50 ºC and dissolved in conc. nitric acid (100 μL) with heating at 90 ºC. Each sample was diluted to 10 mL with deionised water and sent for metal analyses using Inductively-Coupled Plasma Mass Spectrometry at the School of Earth Sciences, The University of Queensland. Cu levels were normalised to protein content. Intracellular Cu concentrations (in nM) were calculated using the assumption that the protein concentration inside an *E. coli* cell is ~300 mg/mL. **(B) Fold increase in intracellular Cu levels.** This was calculated using data from panel (A). **(A-B)** Results were averaged from five independent experiments. Error bars represent ± SD.

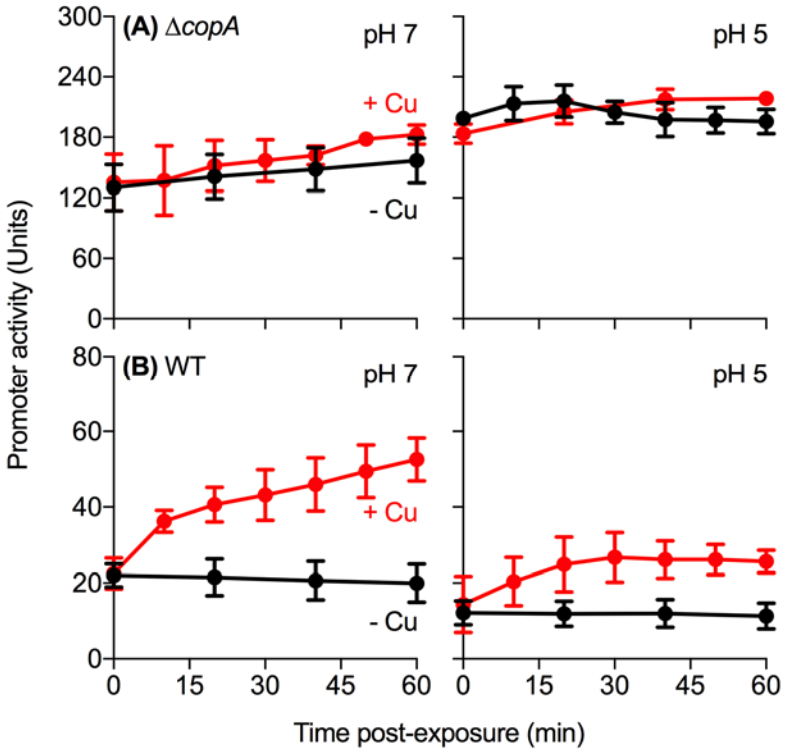

Figure S6. Response of P$_{copA}$-*lacZ* reporter to Cu stress at pH 7 and pH 5. *E. coli* UTI89 **(A)** Δ*copA* mutant and **(B)** WT strains harbouring the P$_{copA}$-*lacZ* plasmid were cultured at pH 7 or pH 5 without any added Cu. Upon reaching the mid-exponential phase, bacteria were challenged with water (-Cu, black traces) or 1 µM of added Cu (+Cu, red traces) in the same medium. Bacteria were collected at intervals up to 60 min post-exposure. β-galactosidase activities were measured following standard protocol using *o*-nitrophenyl-β-galactoside (1 mg/mL) as substrate. The total volume of each sample was 200 µL. Absorbance values at 420 nm were recorded in microtitre plates and results were expressed as Miller units. Data were averaged from three independent experiments. Error bars represent ± SD.

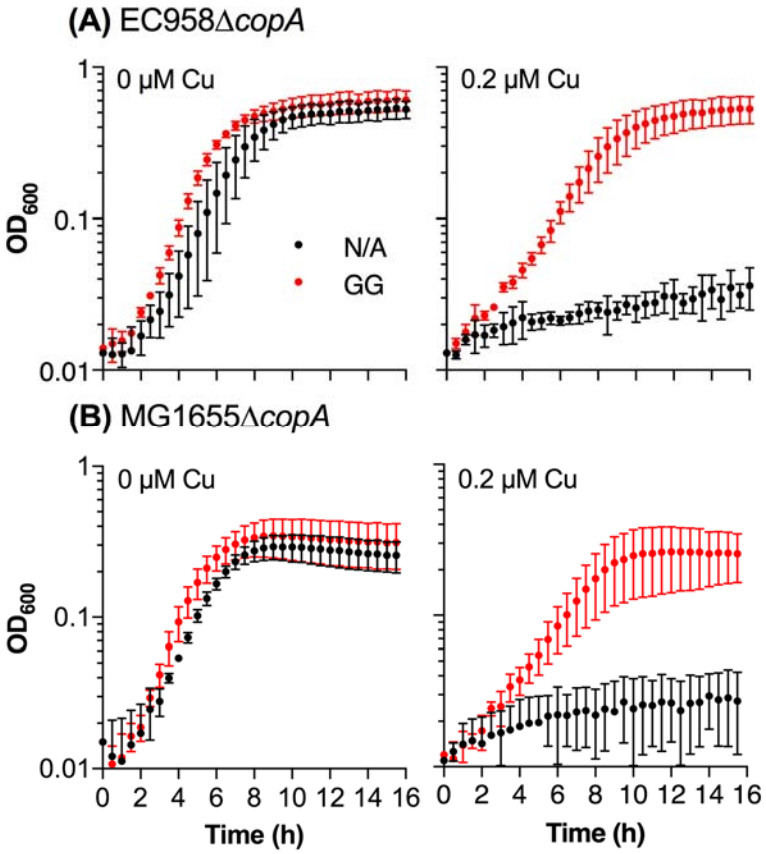

Figure S7. Protective effects of Glu and Gln in different *E. coli* strains. *E. coli* **(A)** EC958Δ*copA* and **(B)** MG1655Δ*copA* mutant strains were cultured at pH 5 in the presence of 0 or 0.2 μM added Cu. The medium was supplemented with water (black, N/A) or a combination of Glu and Gln (0.25 mM each, red, GG). Data were averaged from three independent experiments. Error bars represent ± SD.

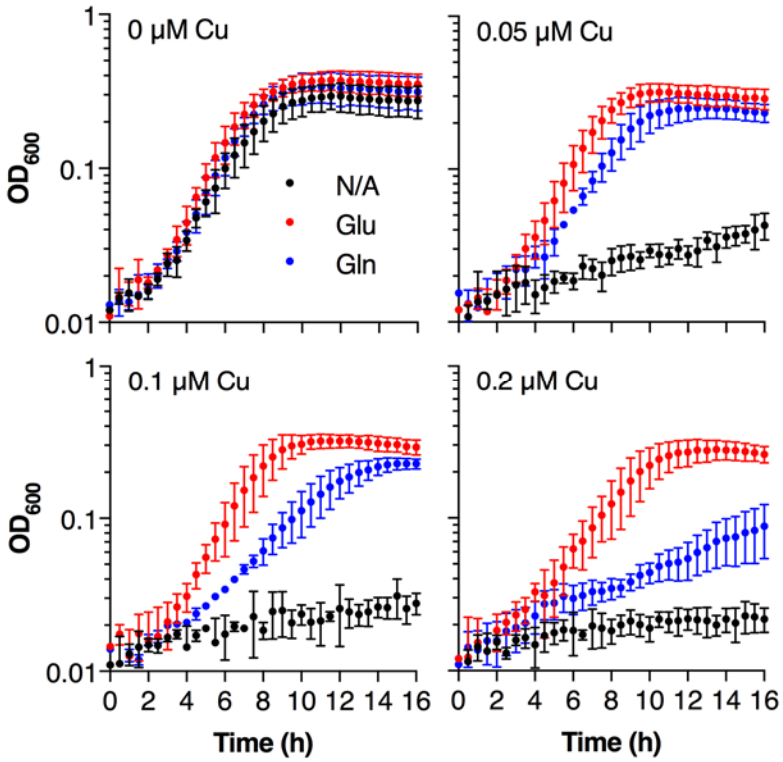

Figure S8. Separate protective effects of Glu and Gln. *E. coli* UTI89Δ*copA* mutant strain was grown at pH 5 in the presence of 0 – 0.2 µM added Cu. The culture medium was supplemented with water (black), 0.5 mM Glu (red), or 0.5 mM Gln (blue). Data were averaged from three independent experiments. Error bars represent ± SD.

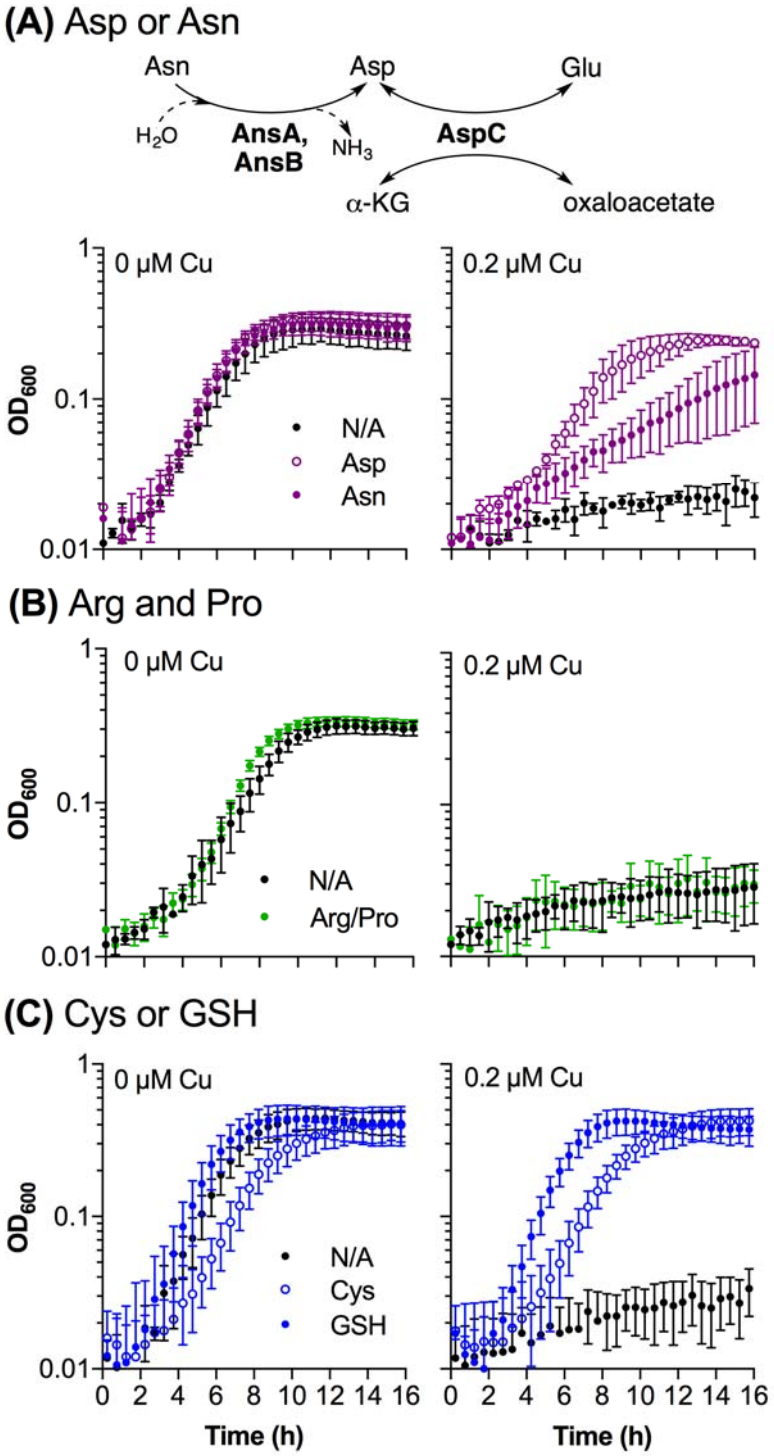

Figure S9. Protective effects of (A) Asp or Asn, (B) Arg and Pro, (C) Cys or GSH. *E. coli* UTI89Δ*copA* mutant strain was cultured at pH 5 in the presence of 0 or 0.2 μM added Cu. The medium was supplemented with water (N/A, black circles) or 0.5 mM of each amino acid as indicated. Data were averaged from three independent experiments. Error bars represent ± SD. Pathway for the generation of Glu from Asn and Asp *via* the two asparaginases in *E. coli* (AnsA and AnsB) and aspartate aminotransferase (AspC) was shown in panel (A).

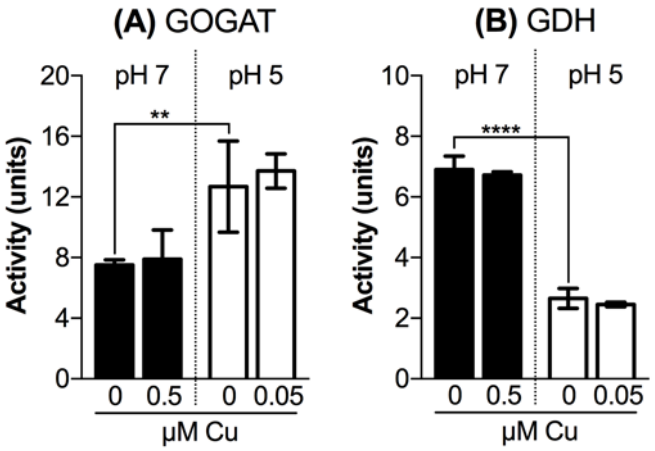

Figure S10. Effects of Cu on the activities of glutamate-synthesising enzymes in WT bacteria. UTI89 WT was cultured at pH 7 (black columns) in the presence of 0 or 0.5 µM Cu, or at pH 5 (white columns)in the presence of 0 or 0.05 µM Cu. Mid-exponential cells were collected and activities of **(A)** GOGAT and **(B)** GDH were measured in cell-free lysis extracts. Data were averaged from three independent experiments. Error bars represent ± SD. GOGAT activities were reproducibly higher in bacteria cultured at pH 5 ($^{**}P < 0.01$) while GDH activities were higher in bacteria cultured at pH 7 ($^{****}P < 0.0001$).

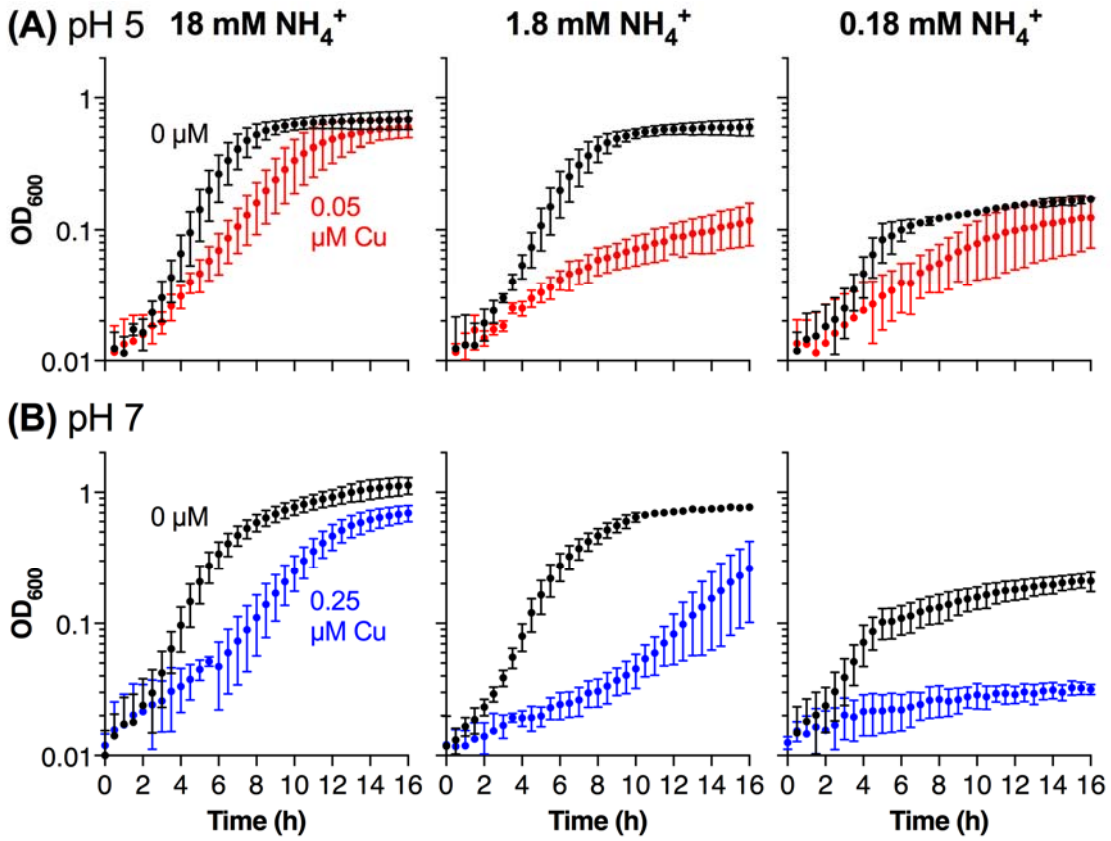

Figure S11. Effects of ammonia availability on Cu stress. *E. coli* UTI89Δ*copA* mutant strain was grown at **(A)** pH 5 or **(B)** pH 7 with or without Cu as indicated. The culture medium contained 18, 1.8, or 0.18 mM ammonium chloride as the sole nitrogen source. Data were averaged from four independent experiments. Error bars represent ± SD.

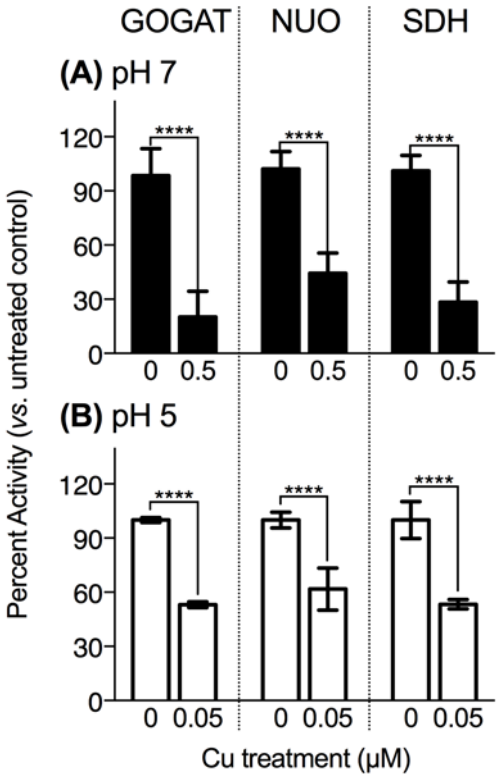

Figure S12. Effects of Cu on the activities of iron-sulfur enzymes. *E. coli* UTI89Δ*copA* mutant strain was cultured **(A)** at pH 7 in the presence of 0 or 0.5 μM added Cu or **(B)** at pH 5 in the presence of 0 or 0.05 μM added Cu. Mid-exponential cells were collected and activities of GOGAT, NUO, and SDH were measured in cell-free lysis extracts. Results were normalised to the untreated control (cultured with 0 μM added Cu). Data were averaged from three independent experiments. Error bars represent ± SD. $^{****}P < 0.0001$.

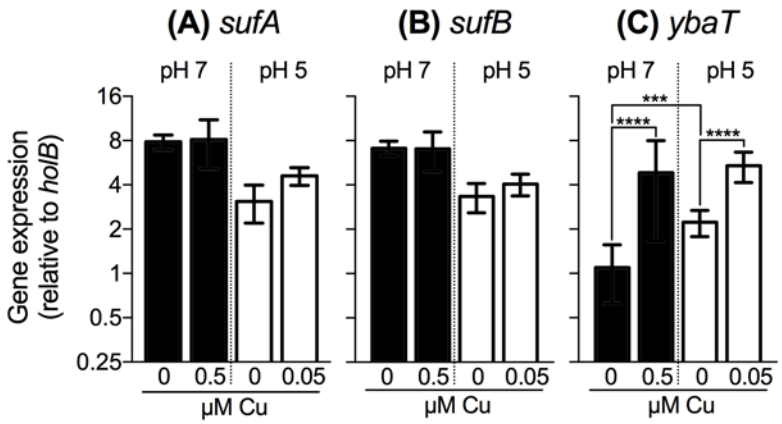

Figure S13. Effects of Cu on expression of (A) *sufA*, (B) *sufB*, and (C) *ybaT*. *E. coli* UTI89Δ*copA* mutant strain was cultured at pH 7 (black columns) or in the presence of 0 or 0.5 µM Cu at pH 5 (white columns) in the presence of 0 or 0.05 µM Cu. Total RNA was extracted from mid-exponential cells and amounts of transcripts relative to *holB* were measured by qPCR. Data were averaged from six independent experiments. Error bars represent ± SD from the mean. $^{***}P < 0.001$, $^{****}P < 0.0001$.

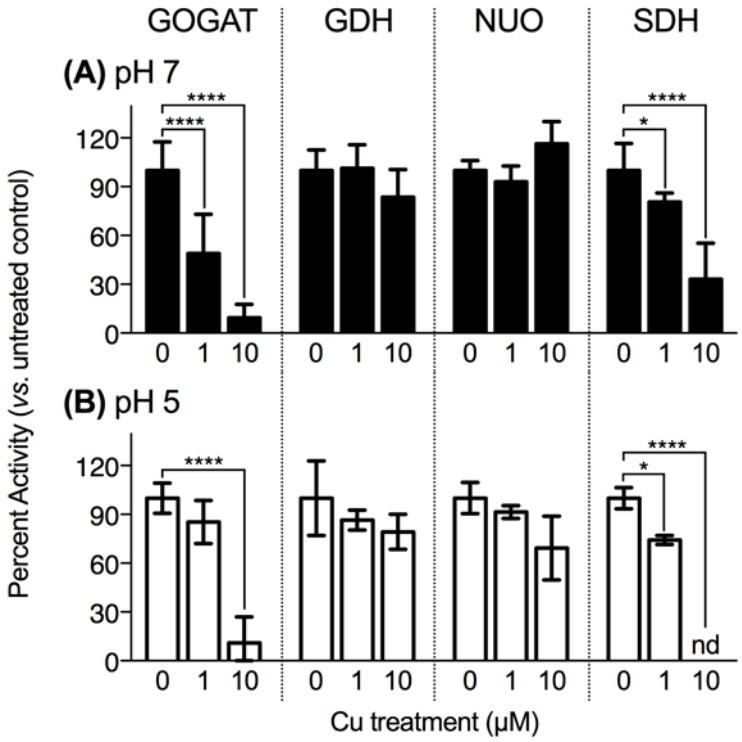

Figure S14. Excess Cu ions may directly damage GOGAT. *E. coli* UTI89Δ*copA* mutant strain was cultured at **(A)** pH 7 or **(B)** pH 5 without any added Cu to the mid-exponential phase and was subsequently challenged with 0, 1, or 10 μM Cu. After 30 min, cells were collected and activities of GOGAT, GDH, NUO, and SDH were measured in cell-free lysis extracts. Data were averaged from three independent experiments. Error bars represent ± SD. $^{****}P < 0.0001$, $^{*}P < 0.05$.

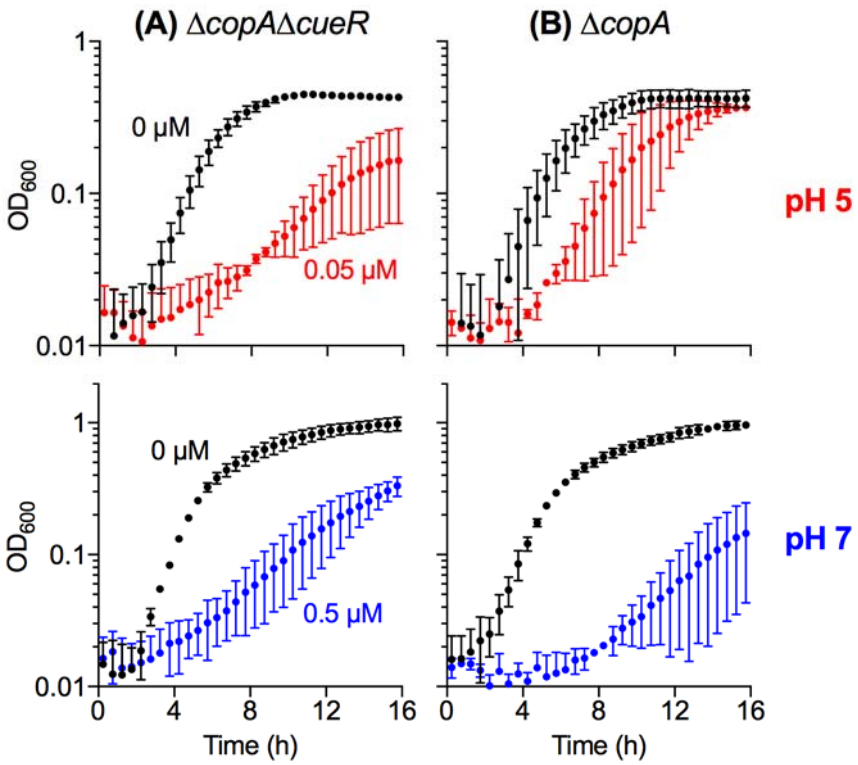

Figure S15. Cu stress in the UTI89Δ*copA*Δ*cueR* mutant. Bacteria were cultured at pH 5 in the presence of 0 or 0.05 μM of added Cu (top panels) or at pH 7 in the presence of 0 or 0.5 μM of added Cu (bottom panels). Data were averaged from three independent experiments. Error bars represent ± SD. Cu stress in the UTI89Δ*copA* parent mutant was assessed in parallel and the results were shown for comparison.

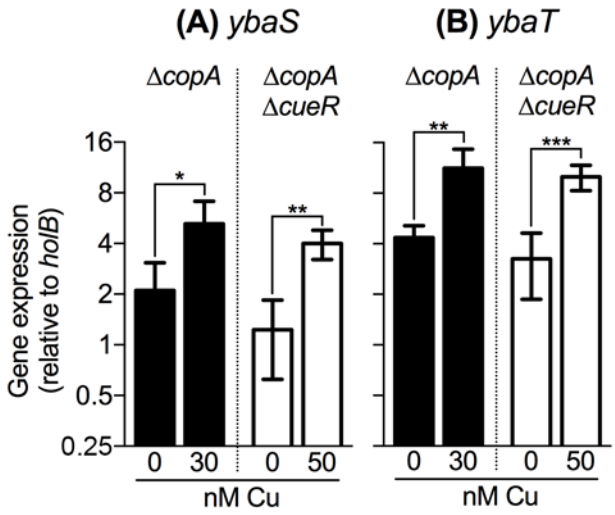

Figure S16. Effects of Cu on expression of (A) *ybaS* and (B) *ybaT* in the UTI89Δ*copA*Δ*cueR* mutant. Bacteria were cultured at pH 5 in the presence of 0, 30, or 50 nM of added Cu as indicated. Data were averaged from three independent experiments. Error bars represent ± SD. $^{*}P < 0.05$, $^{**}P < 0.01$, $^{***}P < 0.001$. Results from parallel experimentation with the UTI89Δ*copA* parent mutant strain were shown for comparison.

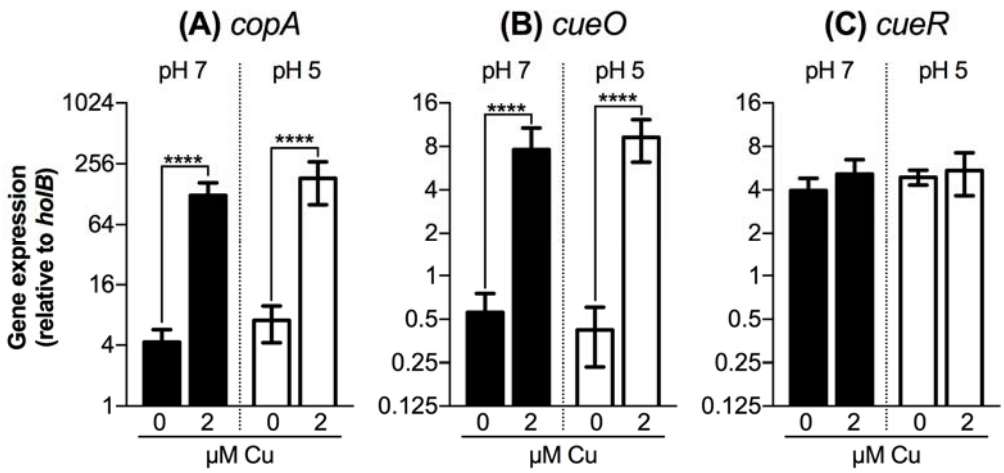

Figure S17. Effects of pH on the expression of Cu tolerance genes in WT cells. The UTI89 WT strain was cultured at pH 7 (black columns) or pH 5 (white columns) in the presence of 0 or 2 µM Cu. Total RNA was extracted from mid-exponential cells and amounts of **(A)** *copA*, **(B)** *cueO*, and **(C)** *cueR* transcripts relative to *holB* were measured by qPCR. Data were averaged from six independent experiments. Error bars represent ± SD from the mean. $^{****}P < 0.0001$.

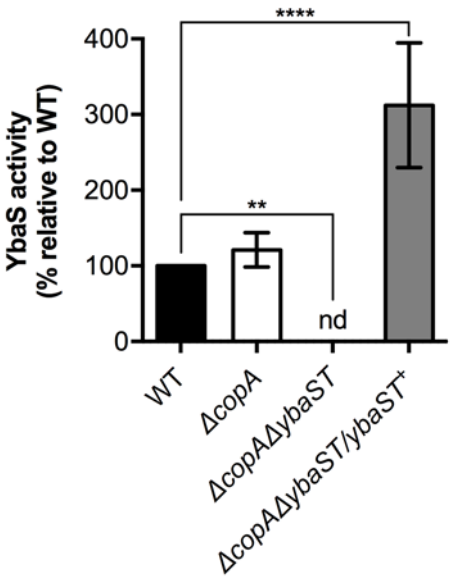

Figure S18. YbaS activity in Δ*ybaST* mutant strains. Bacteria were propagated on Cu-free LB agar overnight and cells from the agar plate were harvested and lysed. YbaS activities were measured in cell-free lysis extracts. Results were normalised to the WT. Data were averaged from three independent experiments. Error bars represent ± SD. nd, not detectable (below detection limit). $^{****}P < 0.0001$, $^{**}P < 0.01$.

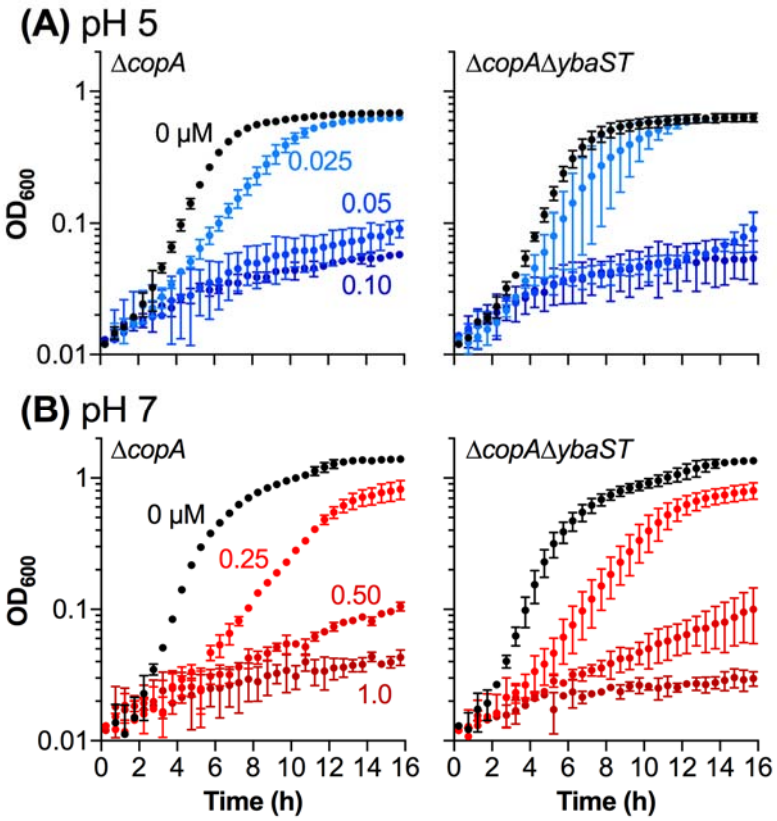

Figure S19. Cu stress in the Δ*copA*Δ*ybaST* mutant strain. Growth of EC958Δ*copA* and Δ*copA*Δ*ybaST* mutant strains **(A)** at pH 5 in the presence of 0 – 0.10 μM of added Cu and **(B)** at pH 7 in the presence of 0 – 1.0 μM of added Cu. Data were averaged from three independent experiments. Error bars represent ± SD.

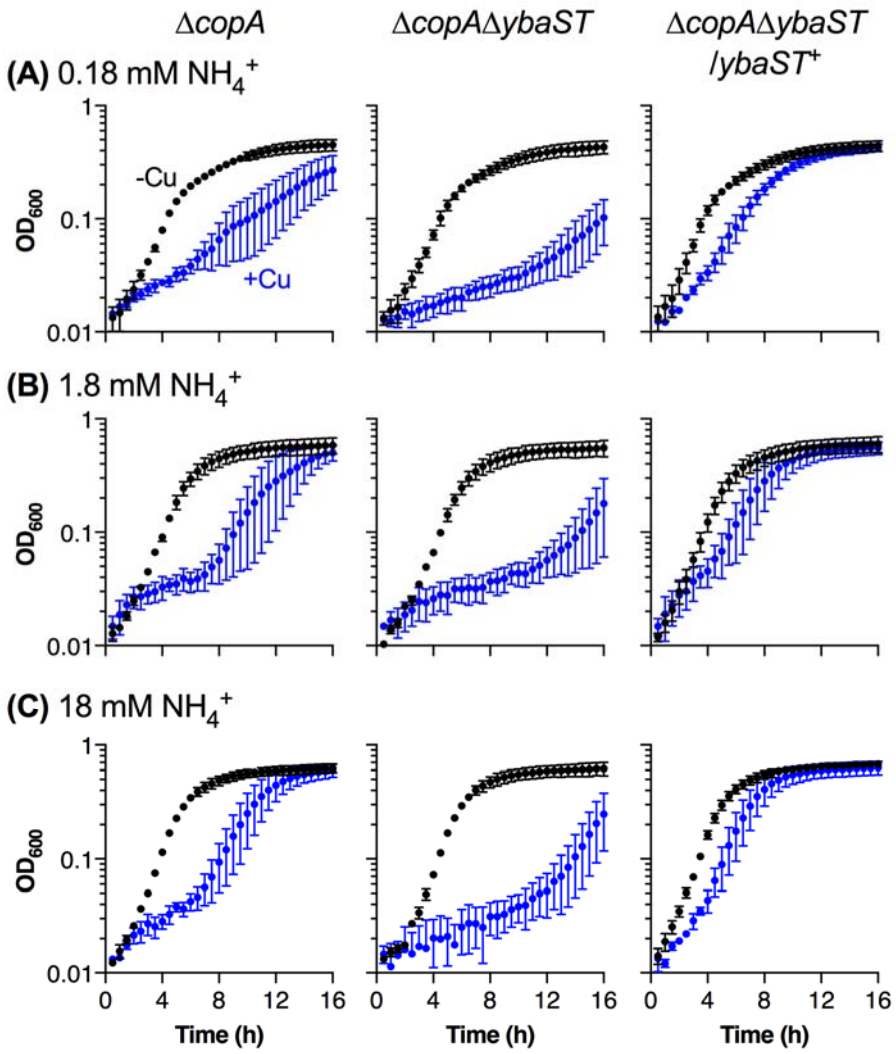

Figure S20. Effects of ammonia availability on Cu stress in the Δ*copA*Δ*ybaST* mutant. *E. coli* EC958 Δ*copA* mutant, Δ*copA*Δ*ybaST* double mutant, and Δ*copA*Δ*ybaST*/*ybaST*$^{+}$ complemented mutant strain was cultured at pH 5 with 0 (-Cu, black traces) or 0.05 µM of added Cu (+Cu, blue traces). The culture medium contained 0.5 mM Gln and **(A)** 0.18, **(B)** 1.8, or **(C)** 18 mM ammonium chloride. Data were averaged from three independent experiments. Error bars represent ± SD.